Empirical-Statistical Downscaling of Russian and Norwegian temperature series

Rasmus E. Benestad

Locations
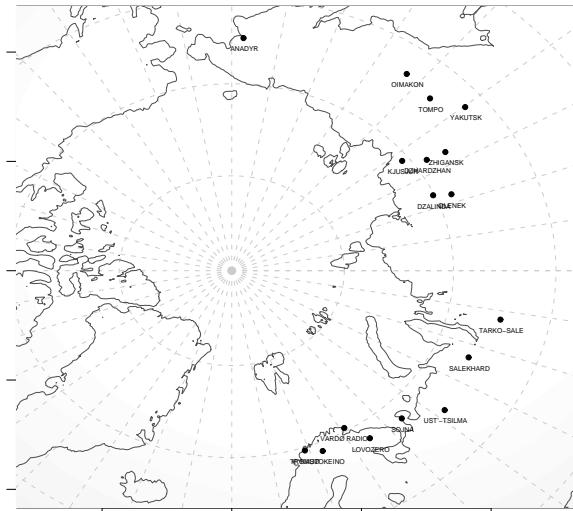
Norwegian Meteorological Institute
met.no

report

Title	Date
Empirical-Statistical Downscaling of Russian and Norwegian temperature series	September 4, 2008
Section Climate	**Report no.** 13/2008
Author R.E. Benestad	**Classification** ● Free ○ Restricted
	ISSN 1503-8025
	e-ISSN 1503-8025
Client(s) The Norwegian Research Council & The Norwegian Meteorological Institute	**Client's reference**

Abstract

Empirical-Statistical downscaling of monthly mean temperature has been carried out for a selection of Russian and Norwegian sites, based on the most recent global climate model simulations described in the Intergovernmental Panel on Climate Change (IPCC) fourth assessment report (AR4) from 2007. The downscaling analysis incorporated multi-model ensembles based on 47 integrations following the SRES A1b emission scenario, although poor results for some sites were discarded. All sites suggest a significant future warming, with seasonal mean temperatures increasing by 1.7–10.1°C by 2070–2099. For most of the Russian sites east of 80°E, the strongest projected warming is estimated for the autumn, whereas for the Norwegian and west Russian sites, winter or spring is expected to warm fastest.

Keywords

Empirical-Statistical downscaling, Russian temperature series, Climate change scenarios.

Disciplinary signature	Responsible signature
Inger Hanssen-Bauer	Eirik Førland

Contents

1   Introduction

The objective of this report is primarily to document a set of calculations done for various International Polar Year (IPY[1]) projects (e.g. EALAT[2] and CAVIAR[3]). The focus will be on the methodological details and the results. However, a short introduction to background is also provided for the readers who are new to the subject. The lay out of the report is as follows: a brief introduction, description of the data, methods, the results, discussion, conclusion and an appendix.

This report have much in common with *Benestad* (2008b,a); *Engen-Skaugen* et al. (2008, 2007). Hence, the introduction of this report is copied from these earlier reports.

1.1   The problem

Since the industrial revolution, the levels of atmospheric concentrations of long-lived greenhouse gases such as CO_2 have risen (*IPCC*, 1995; *Houghton* et al., 2001; *Solomon* et al., 2007) and the most recent estimate suggests that the global mean surface temperature on Earth has increased by $0.74 \pm 0.18°$C over the last 100 years (*Solomon* et al., 2007). It has been well-known within the scientific community for a long time that the effect of raised levels of atmospheric CO_2 will lead to a surface warming (*Weart*, 2003; *Peixoto & Oort*, 1992; *Fleagle & Businger*, 1980; *Houghton*, 1991; *Solomon* et al., 2007; *Houghton* et al., 2001; *IPCC*, 1995, 1990), and that future increases in the levels of greenhouse gases will warm the surface further (*Meehls* et al., 2007; *Christensen* et al., 2007a).

1.2   Introduction to downscaling

Global Climate models (GCMs) represent the most important tool for simulating Earth's climate, but they do not give a realistic description of the local climate in general (*Benestad* et al., 2008)[4].

Global climate models tend to have a coarse spatial resolution (Figure 1), and are unable to represent aspects with spatial scales smaller than the grid box size. The global climate models are also unable to account for substantial variations in the climate statistics within a small region, such as the temperature differences within a small region. Neither do the GCMs give a

---

[1]http://www.ipy.org/
[2]http://www.arcticportal.org/en/icr/ealat
[3]http://www.cicero.uio.no/projects/detail.aspx?id=30170&lang=EN
[4]Early version of the compendium also available at http://www.gvc2.gu.se/ngeo/rcg/edu/esd.pdf
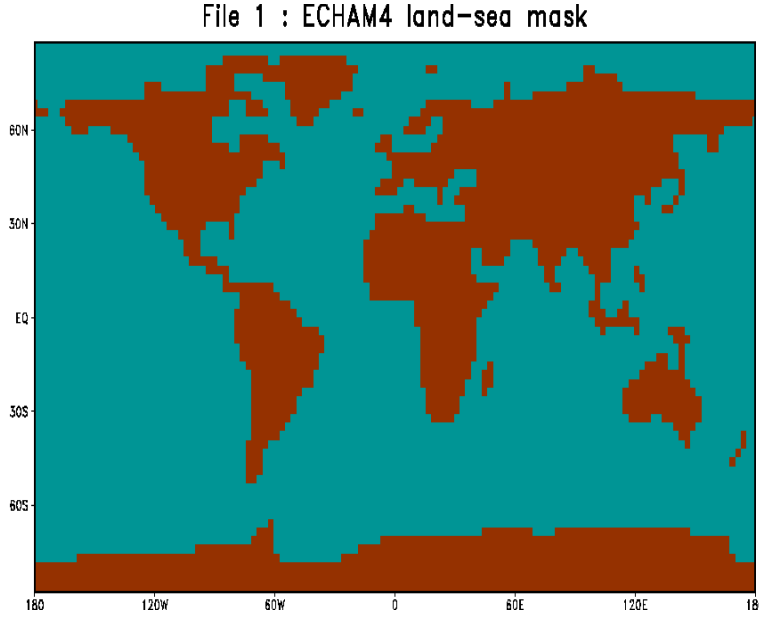
Figure 1: *An example of land-sea mask of a general circulation model (GCM) with* $\sim 2° \times 2°$ *spatial resolution (T42). Notice that Italy and Denmark are not represented in the model.*

perfect description of the real climate system, as they include 'parameterisations' that involve simple statistical models giving an approximate or ad-hoc representation of sub-grid processes.

It is therefore common to downscale the results from the GCMs, either through a (i) nested high-resolution regional climate model (RCM) (*Christensen & Christensen*, 2002; *Christensen* et al., 2001, 1998; *Haugen* et al., 2000; *Haugen & Ødegaard*, 2003) or (ii) through empirical/statistical downscaling (*von Storch* et al., 1993a; *Rummukainen*, 1997; *Easterling*, 1999; *Benestad*, 2004; *Wilby* et al., 2004; *Hanssen-Bauer* et al., 2005; *Fowler* et al., 2007; *Benestad* et al., 2008). The latter is henceforth referred to as 'empirical-statistical downscaling', or the abbreviation 'ESD'.

Here we will define downscaling as *the process of making the link between the state of some variable representing a large space* (henceforth referred to as the 'large scale') *and the state of some variable representing a much smaller space* (henceforth referred to as the 'small scale'.)

Another view of ESD is that it basically is just an advanced statistical analysis of the model results.

The large-scale variable may for instance represent the circulation pattern over a large region whereas the small scale may be the local temperature as measured at one given point (station measurement).

It is important to keep in mind the limitations of statistical downscaling, especially when applied to model results from greenhouse gas (GHG) integrations using GCMs. The statistical models are based on historical data, and there is no guarantee that the past statistical relation-

ships between different data fields will hold in the future.

One should also be concerned about the uncertainties associated with the GCM results as well as those of the downscaling methods themselves (*Wilby* et al., 1998). It is well known that low resolution GCMs are far from perfect, and that they have problems associated with for instance cloud representation, atmosphere-ocean coupling, and artificial climate drift (*Bengtsson*, 1996; *Anderson & Carrington*, 1994; *Treut*, 1994; *Christensen* et al., 2007b).

Part of the problems are due to incomplete understanding of the climate system. The important mechanisms causing variability such as El Niñno Southern Oscillation (ENSO) and the North Atlantic Oscillation (NAO) for instance are probably still not completely understood (*Sarachik* et al., 1996; *Anderson & Carrington*, 1994; *Philander*, 1989; *Christensen* et al., 2007b). Due to discretisation and gridding of data, it is unlikely that the global GCMs will simulate regional details realistically (*Crane & Hewitson*, 1998; *Zorita & von Storch*, 1997; *von Storch* et al., 1993b; *Robinson & Finkelstein*, 1991).

However, because a wide range of global GCMs predict observed regional features (e.g. the NAO, ENSO, the Hadley Cell, atmospheric jets), it is believed that the GCMs may be useful for predicting large scale features.

2   Data

The multi-model ensemble of global climate model (GCM) simulations made with a range of different GCMs, used here and reported in Intergovernmental Panel on climate Change (IPCC) fourth assessment report (AR4) (*Meehl* et al., 2007), are freely available from Program for Climate Model Diagnosis and Intercomparison[5]. This model ensemble includes both simulations for the 20th century (C20) and scenario runs for the 21th century following the Special Report Emission Scenarios (SRES) A1b[6] (*Nakicenovic* et al., 2000). Some of the GCMs have been used to make several parallel runs, differing only by using different initial conditions (starting point).

---

[5] PCMDI; https://esg.llnl.gov:8443/index.jsp

[6] The A1 storyline and scenario family describes a future world of very rapid economic growth, global population that peaks in mid-century and declines thereafter, and the rapid introduction of new and more efficient technologies. Major underlying themes are convergence among regions, capacity building and increased cultural and social interactions, with a substantial reduction in regional differences in per capita income. The A1 scenario family develops into three groups that describe alternative directions of technological change in the energy system. The three A1 groups are distinguished by their technological emphasis: fossil intensive (A1FI), non-fossil energy sources (A1T), or a balance across all sources (A1B) (where balanced is defined as not relying too heavily on one particular energy source, on the assumption that similar improvement rates apply to all energy supply and end-use technologies). (source: `http://www.ipcc.ch/ipccreports/tar/vol4/english/099.htm`)

2.1   Predictors: calibration

Monthly gridded data from the ERA40 (*Bengtsson* et al., 2004; *Simmons & Gibson*, 2000) were used as predictors for training the statistical models.

2.2   Predictors: GCMs

The ESD was applied to the IPCC AR4 (*Meehl* et al., 2007) MMD (also referred to as 'CMIP3') GCM ensemble for both the 20th century and the 21st century simulations separately. Table 2 in the appendix provides a complete list of the GCMs and runs (integrations) included in this analysis. The choice of the GCMs was somewhat arbitrary, as (*i*) results from some models were not available on-line at the time of the downloads, (*ii*) there has been several rounds of fetching GCM data, (*iii*) the impact of adding further GCM results was not expected to add much new information about the inter-model spread, and (*iv*) there was no attempt to have a systematic strategy for a complete set of GCMs and runs (the reason - see points *i–iii*). Nevertheless, the selection of GCMs included in the present analysis represented the most complete set of simulations available at the time of the writing of this report, and most of the CMIP3 GCMs are included in the 'super-ensemble'.

2.3   Predictand

The station data (the predictand) provided by Pavel Svyashchennikov, Arctic and Antarctic research institute (AARI), St. Petersburg State University,Russia, and the locations of the sites are shown in Figure 2.

Some of the predictand data were taken from the Norwegian climate data archive ("KlimaDataVareHuset"), and retrieved using the function `KDVH4DS` in the `R`-package `met.no` (see *R Development Core Team* (2004) for reference to `R`). The Norwegian stations used in the analysis were: 90450, 97250, 98550 and 99730.

3   Methods

3.1   Related work

The method on which these results are based has been used in several previous studies and is therefore well-documented. This study uses similar approach as those used in *Benestad* (2008a) to downscale Norwegian regional climate series and *Engen-Skaugen* et al. (2007) to downscale

Locations
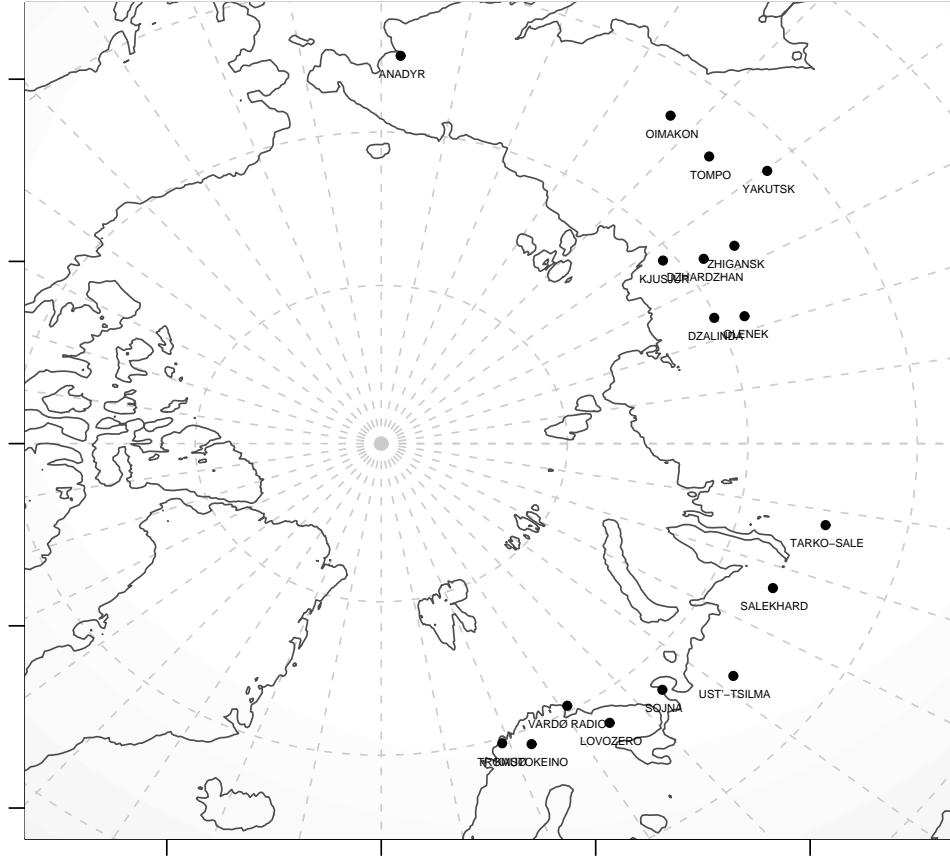
Figure 2: Maps showing the location of the temperature measurements.

river run-off as well as similar analysis where catchment-scale temperature and precipitation were downscaled (*Engen-Skaugen* et al., 2008). Thus, the introduction of those reports are recited here.

The method and the implementation were similar to the work documented in *Benestad* (2005) for each GCM implemented, and performed for monthly mean values. Large-scale temperature was used to downscale the local temperature, as in *Benestad* et al. (2007).

3.2   ESD tool

The tool clim.pact (*Benestad*, 2003a, 2004; *Benestad* et al., 2008) was used to carry out the calculations, using a common empirical orthogonal function (EOF) based framework (*Benestad*, 2001) and linear multiple regression as a basis for the empirical-statistical model.

The ESD was based on a 'finger-print' type technique whereby spatial patterns describing the large-scale anomalies correlated with the local variations were identified in the gridded observations (re-analysis) and then matched with the same spatial structures found in the model results.

3.2.1   Common EOFs & 'finger printing'

A common EOF framework combined large-scale gridded temperature anomalies estimated from the ERA40 re-analysis with corresponding anomalies from a simulation performed by a GCM (interpolated onto the same grid as the former). An ordinary EOF analysis is applied to this combined data set. The common EOF framework yields both the spatial structures (referred to as 'EOFs' or 'modes') as well as weights describing their temporal evolution/variation (referred to as 'principal components').

By combining anomalies rather than the total values, constant biases are removed, however, the constant level of the end results become more arbitrary. Thus, when analysing the final results, it is recommended to focus on trends and long-term transient behaviour rather than the initial level (e.g. the first 10 years) of the downscaled time series.

The principal components (PCs) describing the temporal variations of the different modes (dominant spatial temperature pattern) represent exactly the same spatial structures for GCMs and the ERA40.

3.2.2   ESD model

A step-wise regression analysis was employed that used the part of the PCs describing the ERA40 data together with the predictand (temperature series) to calibrate the model. This calibration returns R^2-statistics, describing how well the run-off can be reproduced with the statistical model if the ERA40 data is used as predictor.

3.2.3   Calibration & assessment

The `clim.pact` tool makes predictions based on the calibration data (here ERA40) as well as the GCM (here either 20th century or the 21st century). However, the ESD-results derived from

ERA40 are not independent and only serves as a visual check of the quality of the statistical downscaling model (not shown here except for in the appendix). The downscaling for the 20th century, on the other hand, provides independent data which can be used in the validation against the actual observations. This validation will test whether the ESD-model is good (here the R^2-statistic is also a measure of skill).

3.2.4 Trend fits

In order to ensure representative values, the downscaled scenarios were adjusted by ensuring that the starting point of the scenarios (SCE) match the final parts of the matching simulations i of the past (CTL). This adjustment was done on calendar month-by-calendar month m basis (e.g. first doing the adjustment for all January months, then for all February months, etc: $y_{i,m,\text{ESD}}(t) = y_{i,m,\text{SCE}}(t) - \overline{y_{i,m,\text{SCE}}(t)} + \overline{y_{i,m,\text{CTL}}(t)}$)), and is performed as default in the `ESD.results()`-call in the `met.no` package version 1.1-0 (June 12 2008) or later. Those runs that did not have a 20th century match were pooled together, and the median of the 3 first years for entire set of unmatched runs were set to the median of the 3 last years of the entire set of 20th century runs.

Note that the adjustment done here differs to that done in *Benestad* (2008a), where rather than matching the 20th and 21st century runs, each of the future scenario runs were adjusted to have the same mean value over overlapping intervals (in *Benestad* (2008a): $y_{\text{m,SCE}}(t) = y_{m,\text{SCE}}(t) - \overline{y_{m,\text{SCE}}(t)} + \overline{y_{m,\text{obs}}(t)}$). Then trends were estimated for the observations and scenarios respectively, taking the best-fit to a fifth-order polynomial for the ensemble median or quantile for the confidence bounds (*Benestad*, 2003b).

3.2.5 Known problems & fixes

Some GCMs had the year wrong in the data files, which has been corrected for in `met.no_1.1-0` (Version: June 12, 2008). The plume plots exclude those GCM runs that give a standard deviation outside the range of $[0.5, 3.0]$ of that of the corresponding observed standard deviation estimated for the time interval 2010–2091 (this is implemented in the `met.no` package version 1.1-0, as of Jun 12 2008).

The series for which there were corresponding runs (here both the GCM and run was matched) for 20th century and the future were stitched together so that the scenario started where the historical run ended.

3.2.6 Quality check

An additional quality control applied to the temperature, for which there was no matching series in the 20C run and the scenario, involved weeding out the time series for which the first mean of the 3 first years (each month was tested individually, thus involving three point averages) was more than 3 standard deviations away from the corresponding ensemble mean for the 3 last corresponding values from the 20C run.

Whereas the predictor domain for most of the stations was automatically defined from objective means within the location of the site $\pm 20°$ of longitude and the latitude $5°$ to the north and $15°$ to the south of the site (however, for some locations, these were relaxed to $\pm 50°$ of longitude and the latitude $10°$ to the north and $30°$ to the south).

The complete listing of the R-script used to make the computations presented here is given in the Appendix.

4   Results

The following figures are shown to provide a quick idea of the main features present in the downscaled results. These should be considered as part of the documentation of these results together with the tables. The results in the figures speak for them selves: there is a general tendency towards warmer climate in the future and there is a considerable spread in the values derived from the different GCM.

In Table 1, the estimated temperature changes (ΔTAM(2070–2099)) were taken as the difference between the observed 1961–1990 climatology and the projected ESD results (as opposed to the boxplots in the appendix, showing the difference between the 1961–1990 C20 simulations and the 2070–2099 SRES A1b values).

Here 'winter' is taken as December–February, 'spring' is March–May, 'summer' June–August, and 'autumn' is September–November.

4.1   Temperature
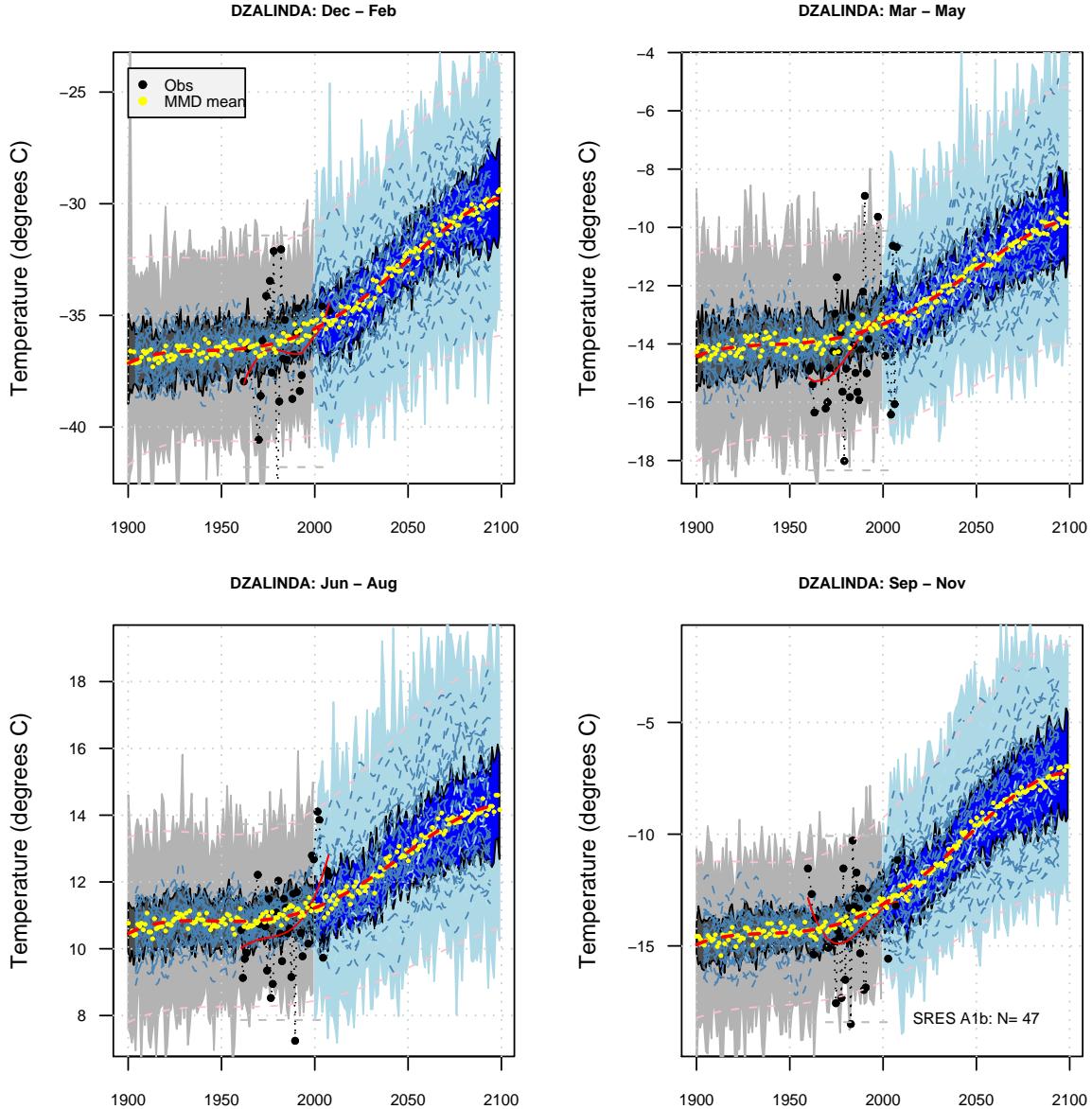
Figure 3: Plume plot for Dzalinda, showing the time evolution of the observed values (black), the 20th Century simulations (grey), and the future scenarios (blue). The light shading shows the minimum–maximum range for the ensemble, and the darker shading marks the inter-quantile range (25%–75%). The yellow symbols mark the ensemble mean values, and the thin red lines show best-fit polynomial to the 5 and 95 percentiles.
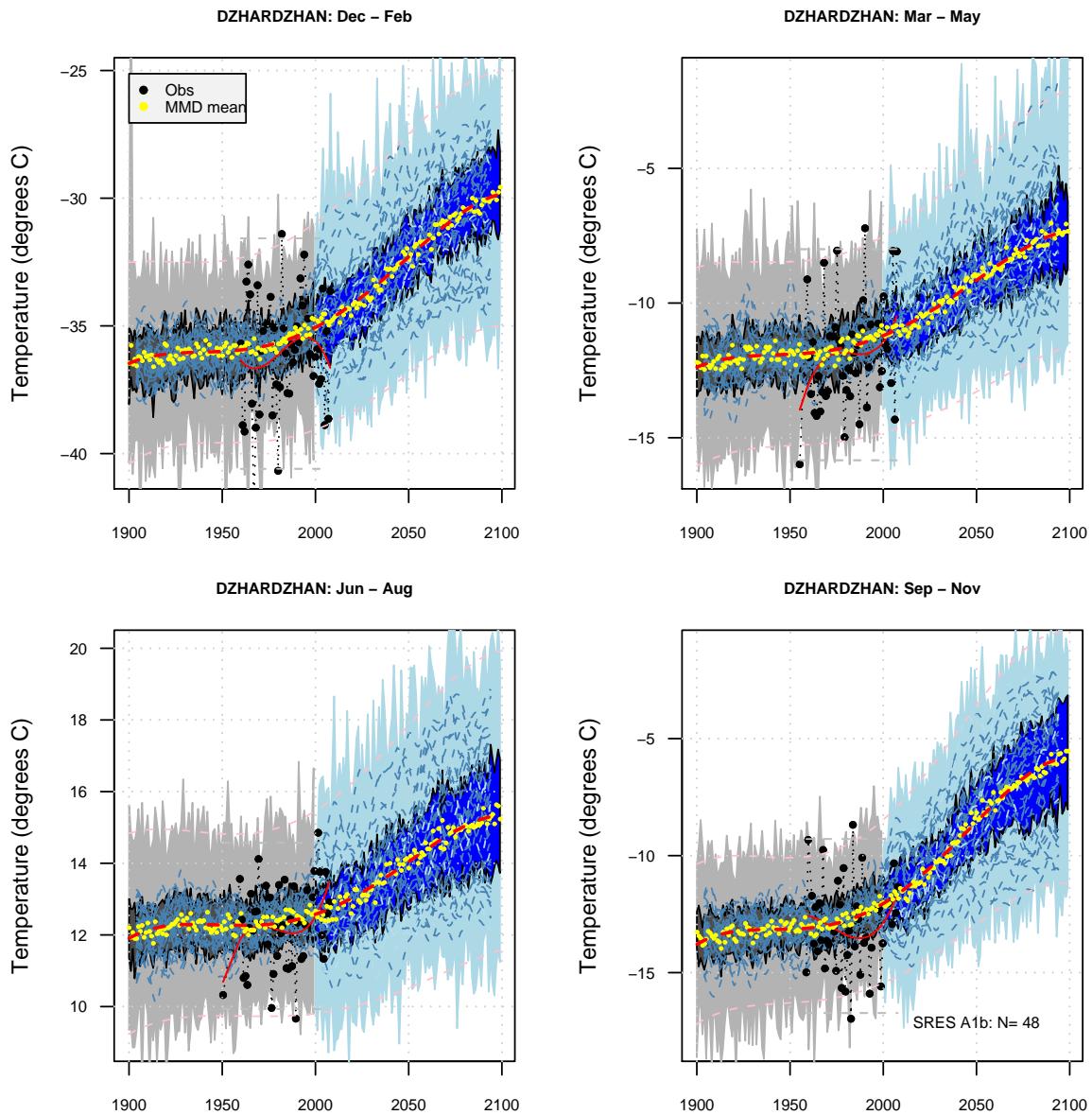
Figure 4: As in Figure 3, but for Dzhardzhan..
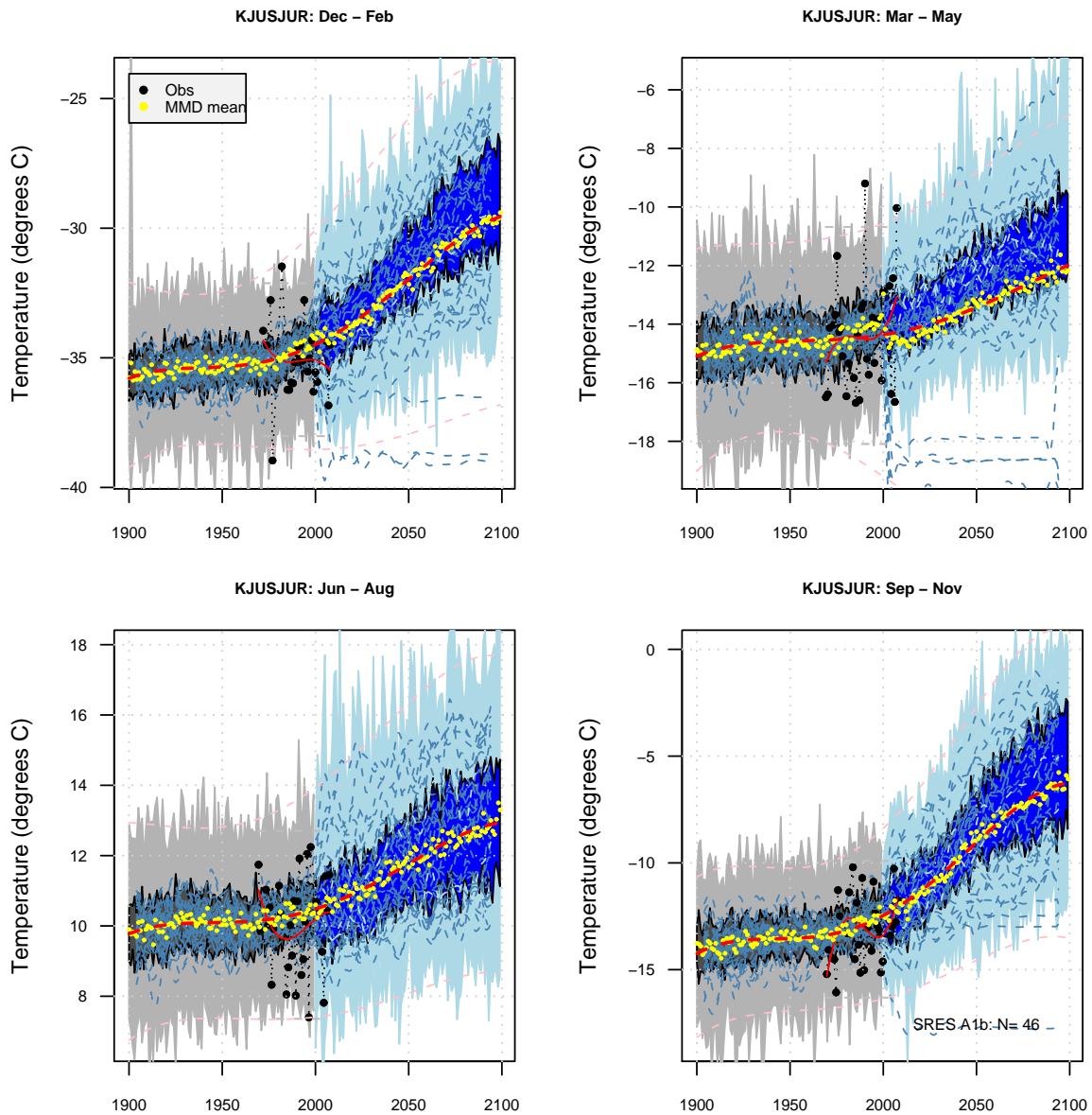
Figure 5: As in Figure 3, but for Kjusur.
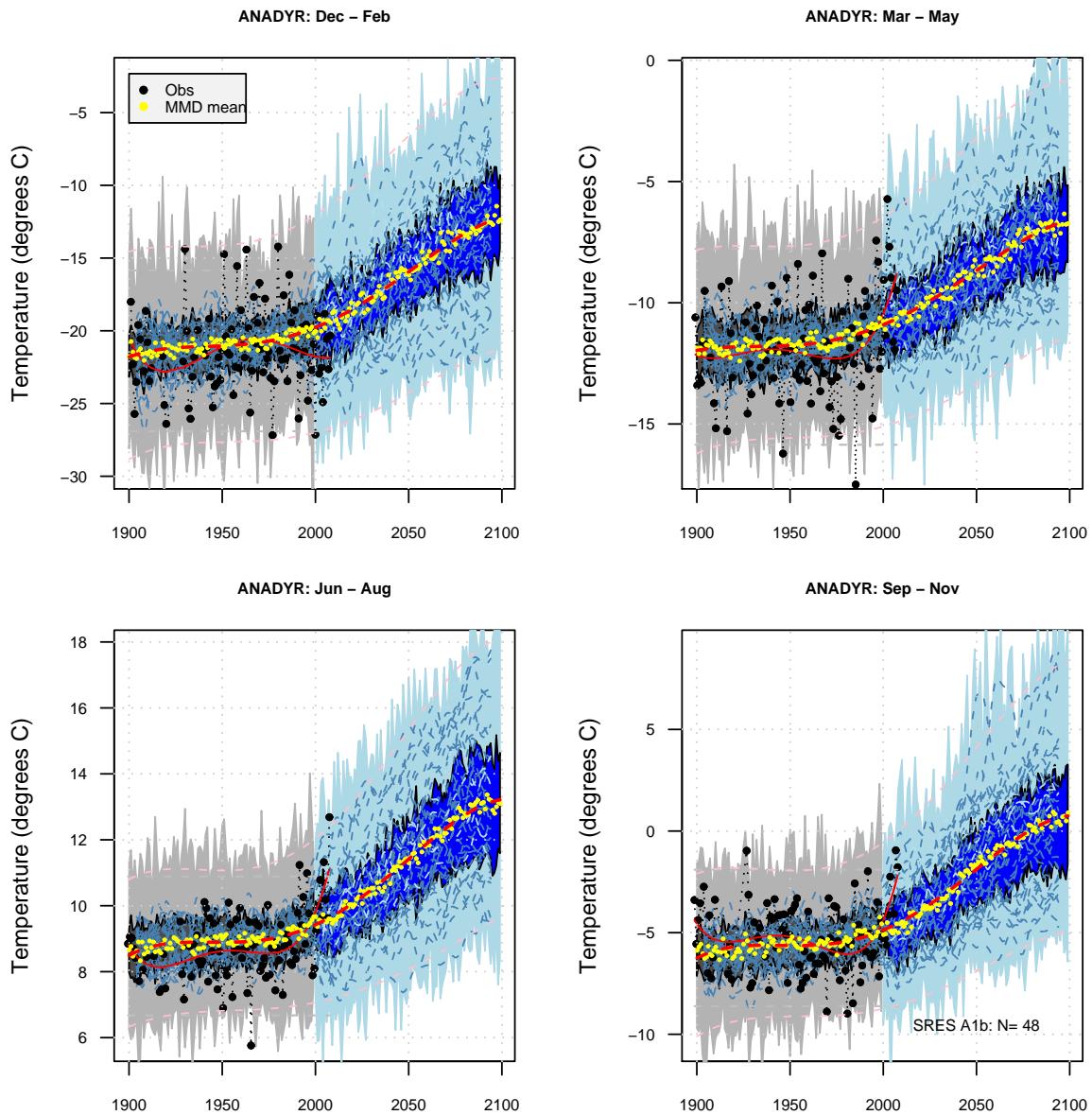
Figure 6: As in Figure 3, but for anadyr.
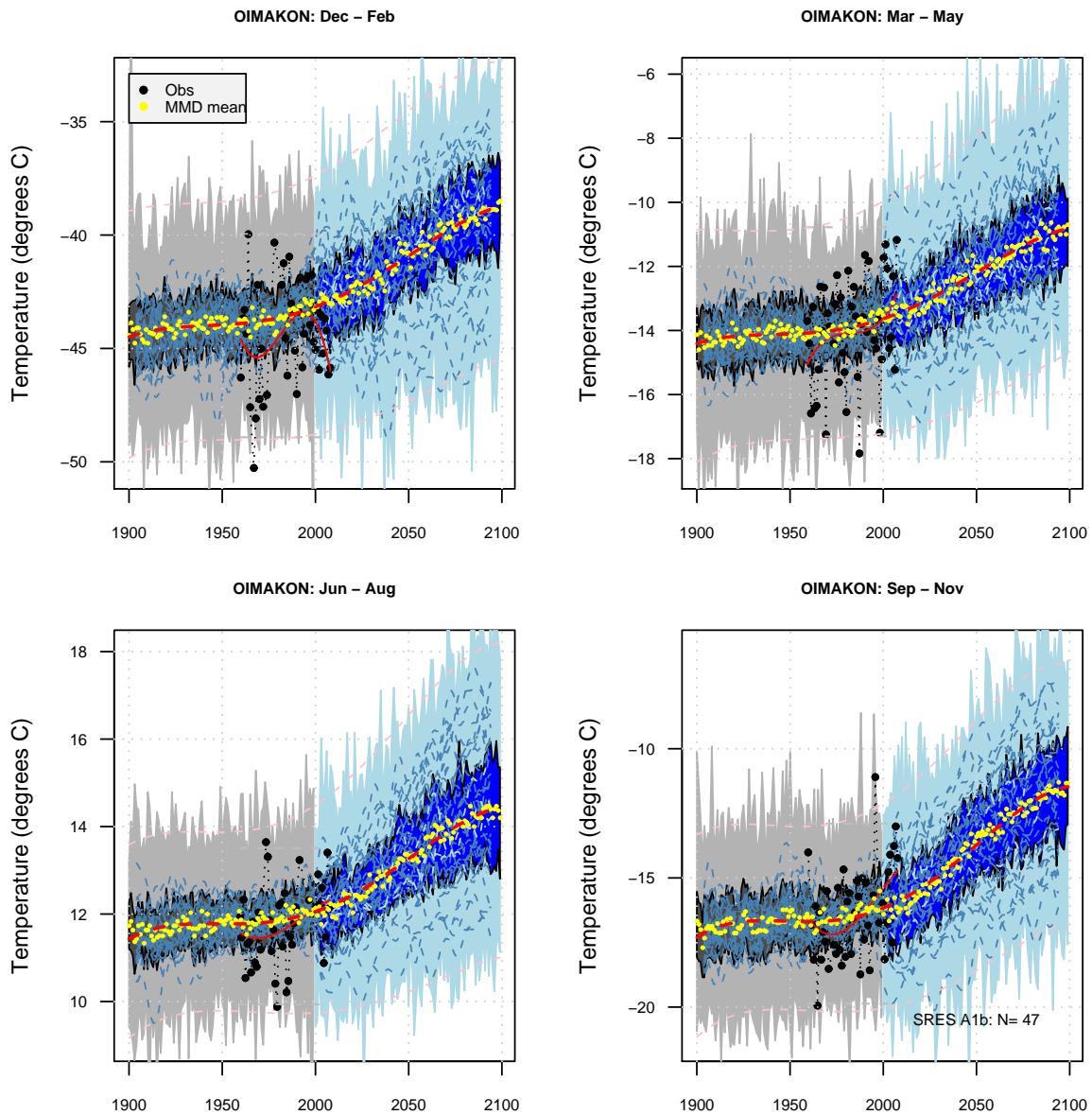
Figure 7: As in Figure 3, but for Oimakon.
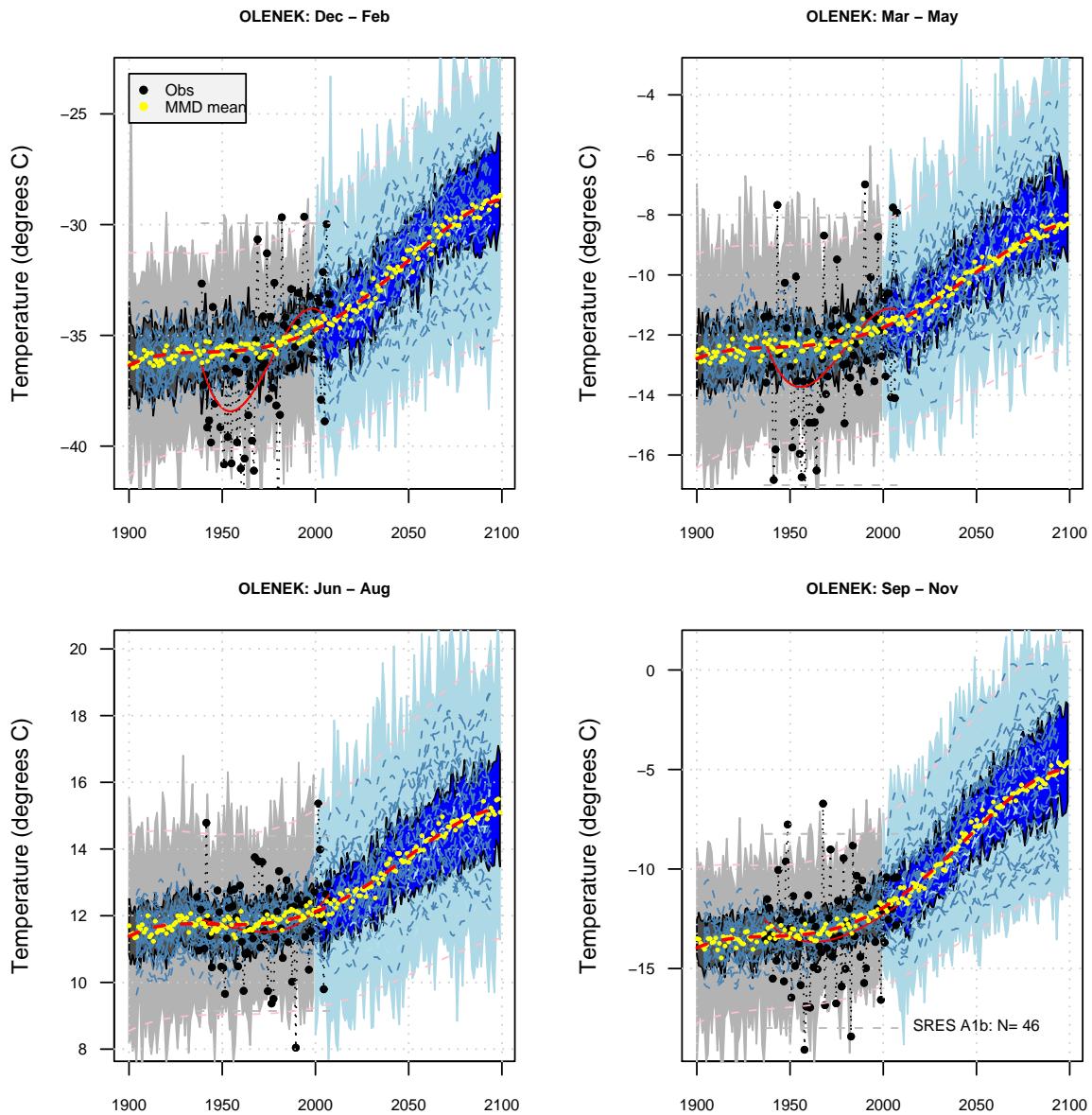
Figure 8: As in Figure 3, but for Olenek.

17
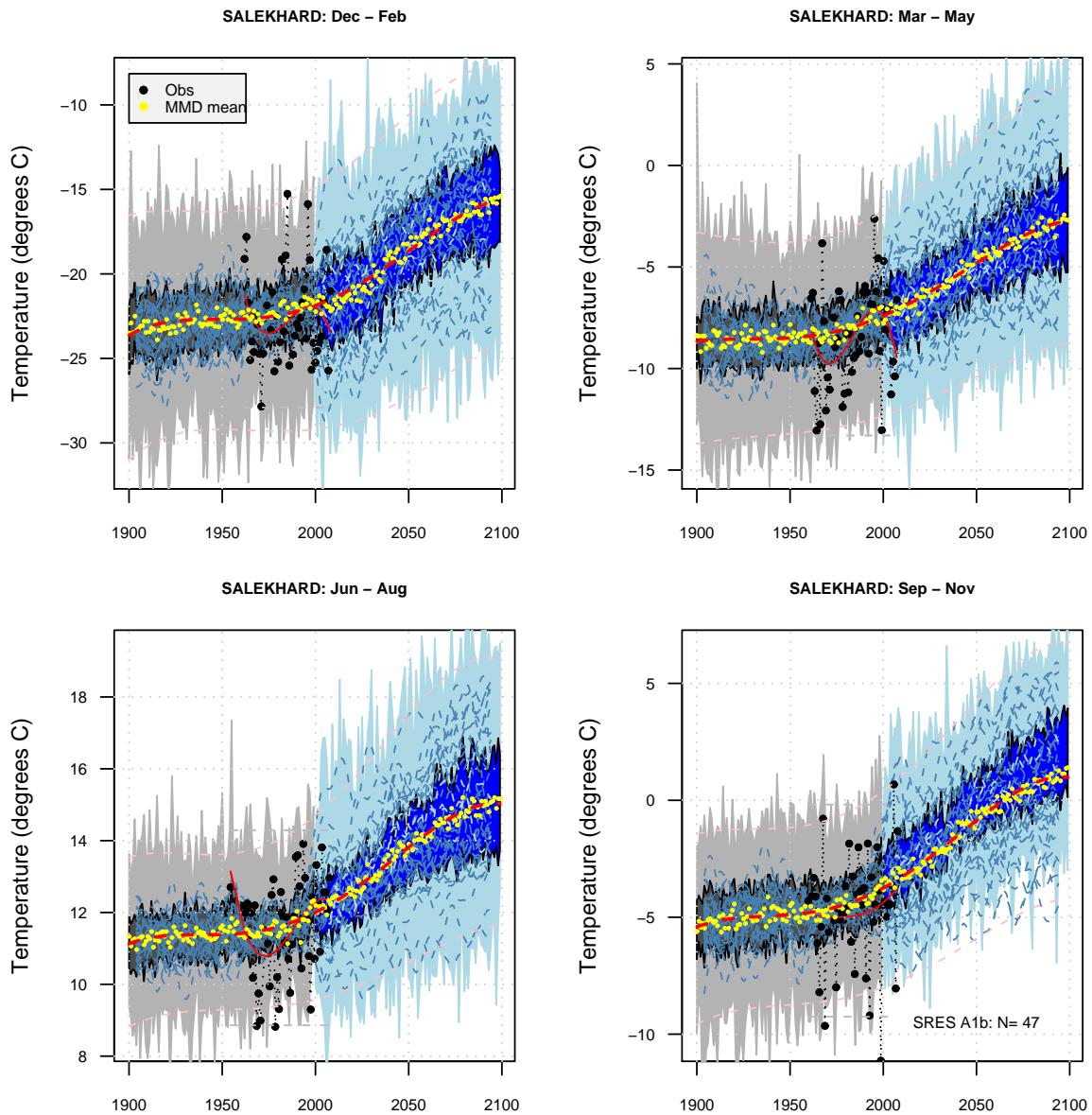
Figure 9: As in Figure 3, but for Salekhard.
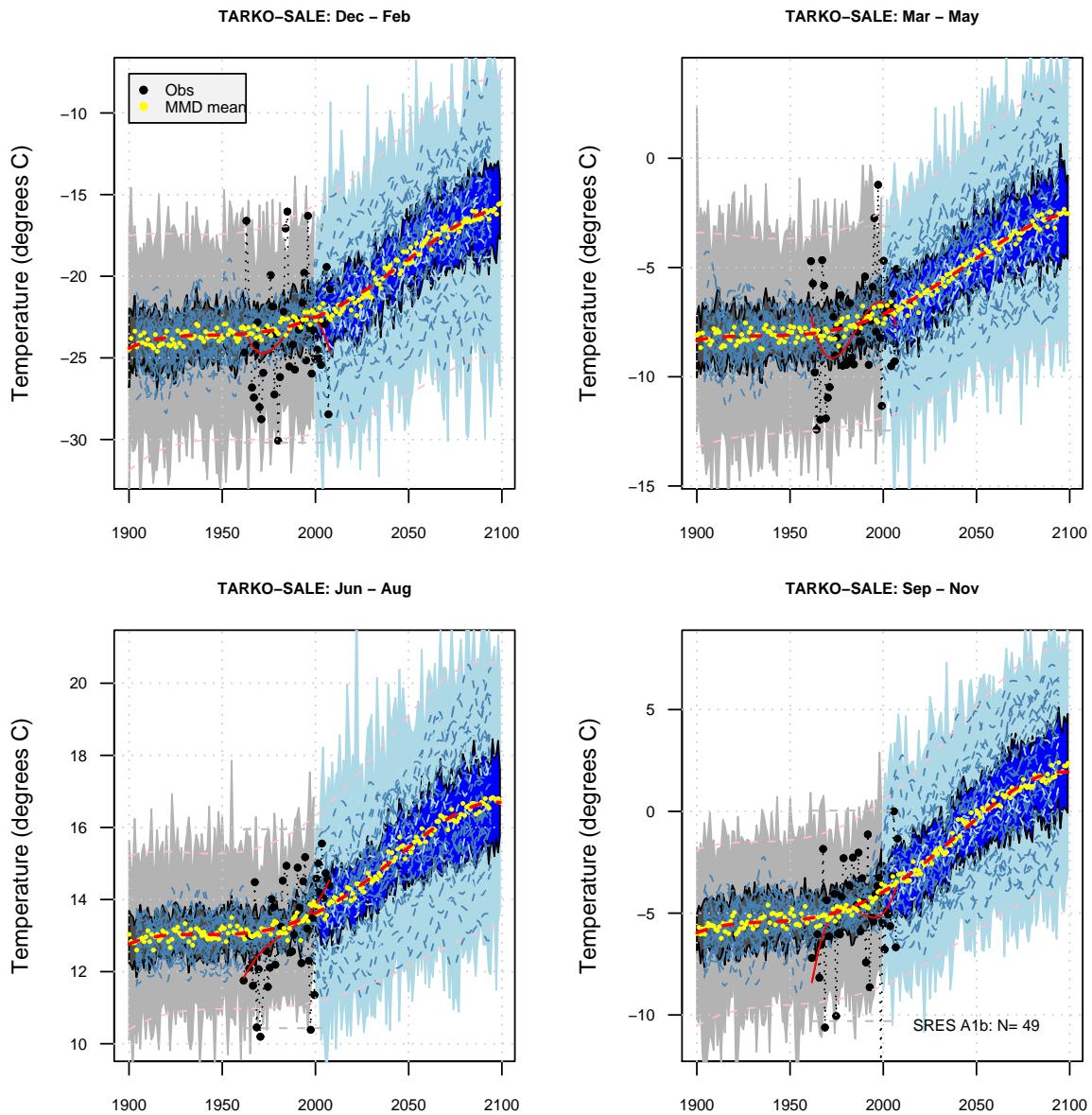
Figure 10: As in Figure 3, but for Tarko-Sale.
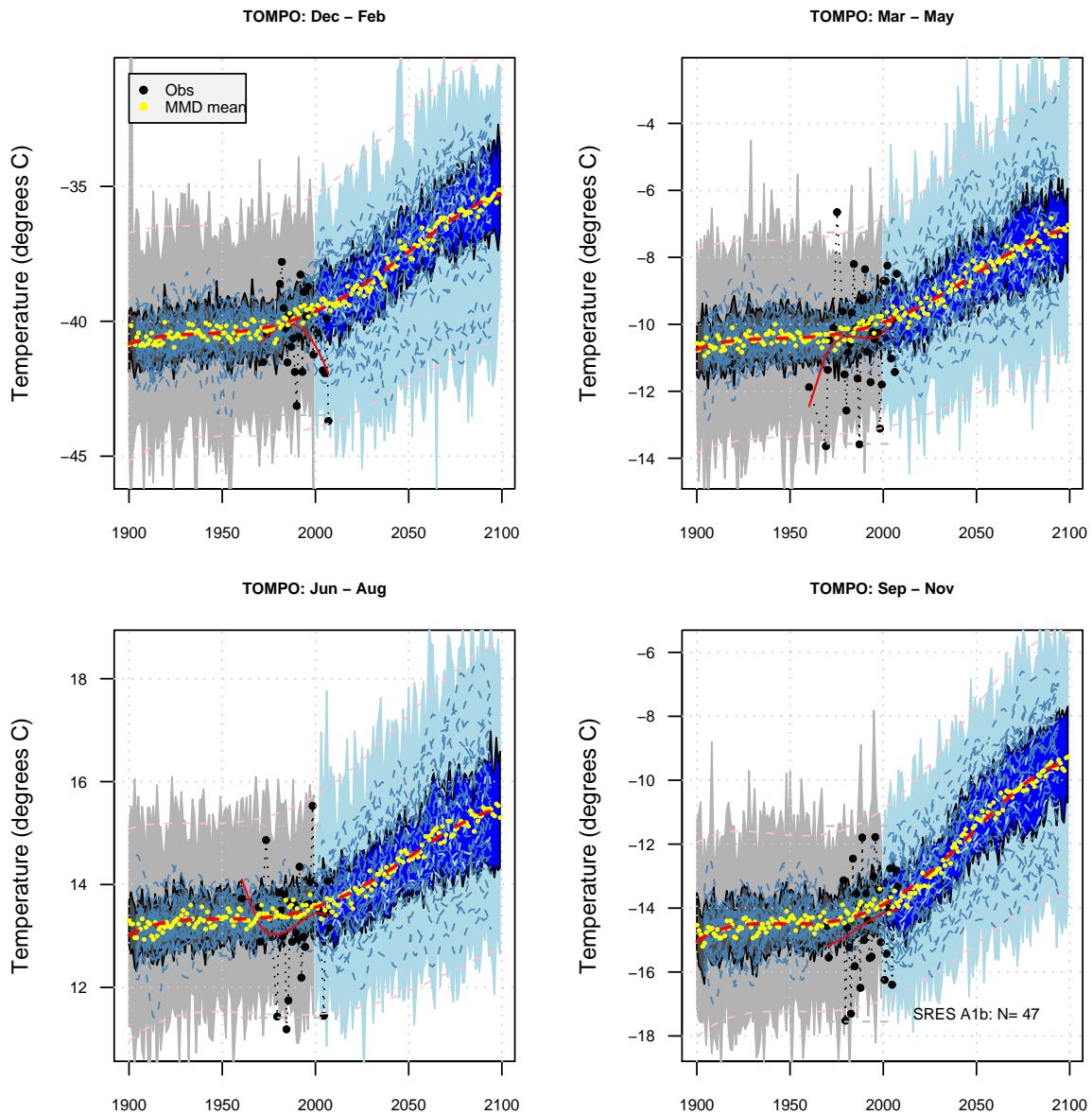
Figure 11: As in Figure 3, but for Tompo.
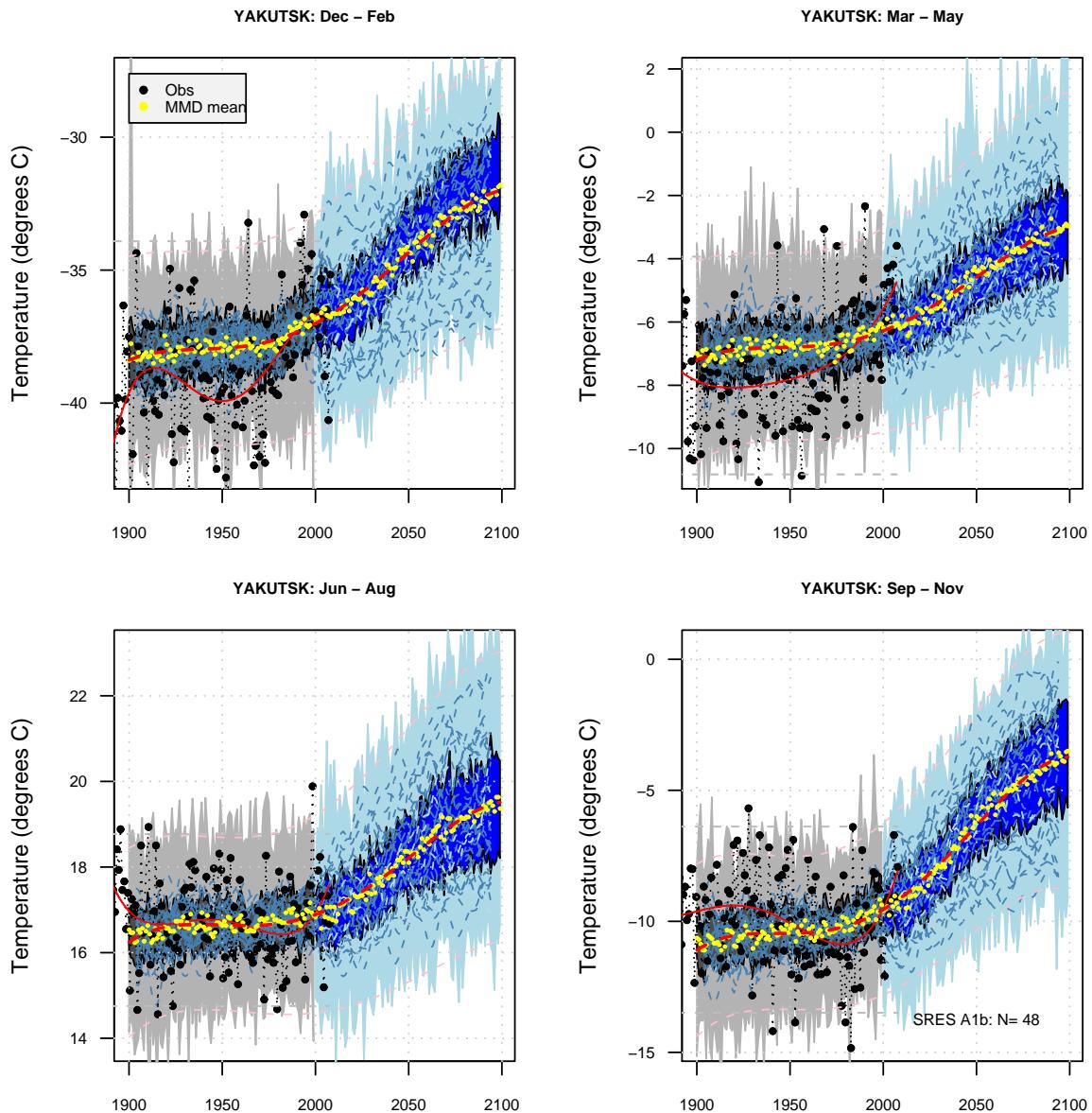
Figure 12: As in Figure 3, but for Yakutsk.

ZHIGANSK: Dec – Feb

ZHIGANSK: Mar – May

ZHIGANSK: Jun – Aug

ZHIGANSK: Sep – Nov

SRES A1b: N= 47
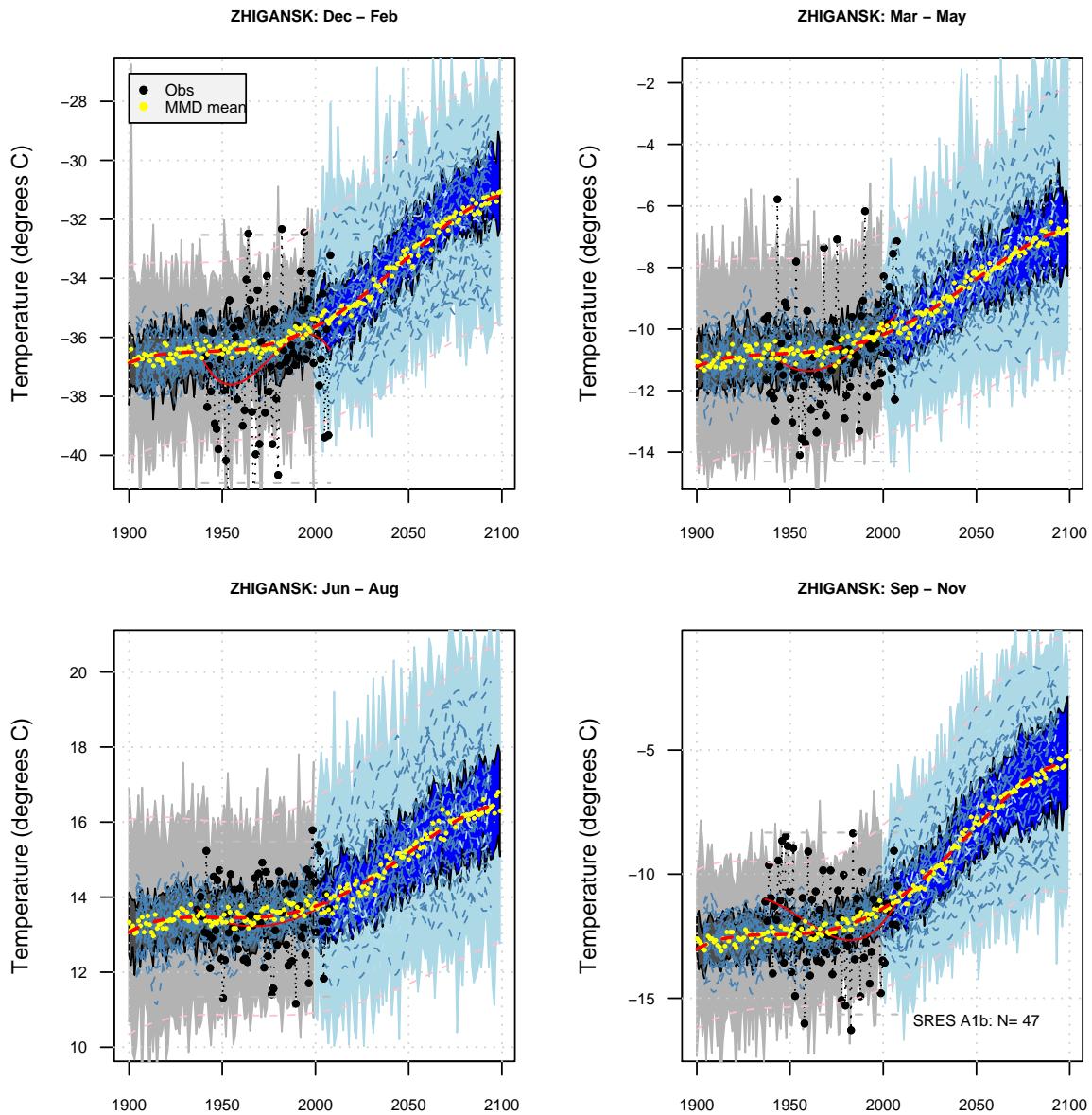
Figure 13: As in Figure 3, but for Zhigansk.
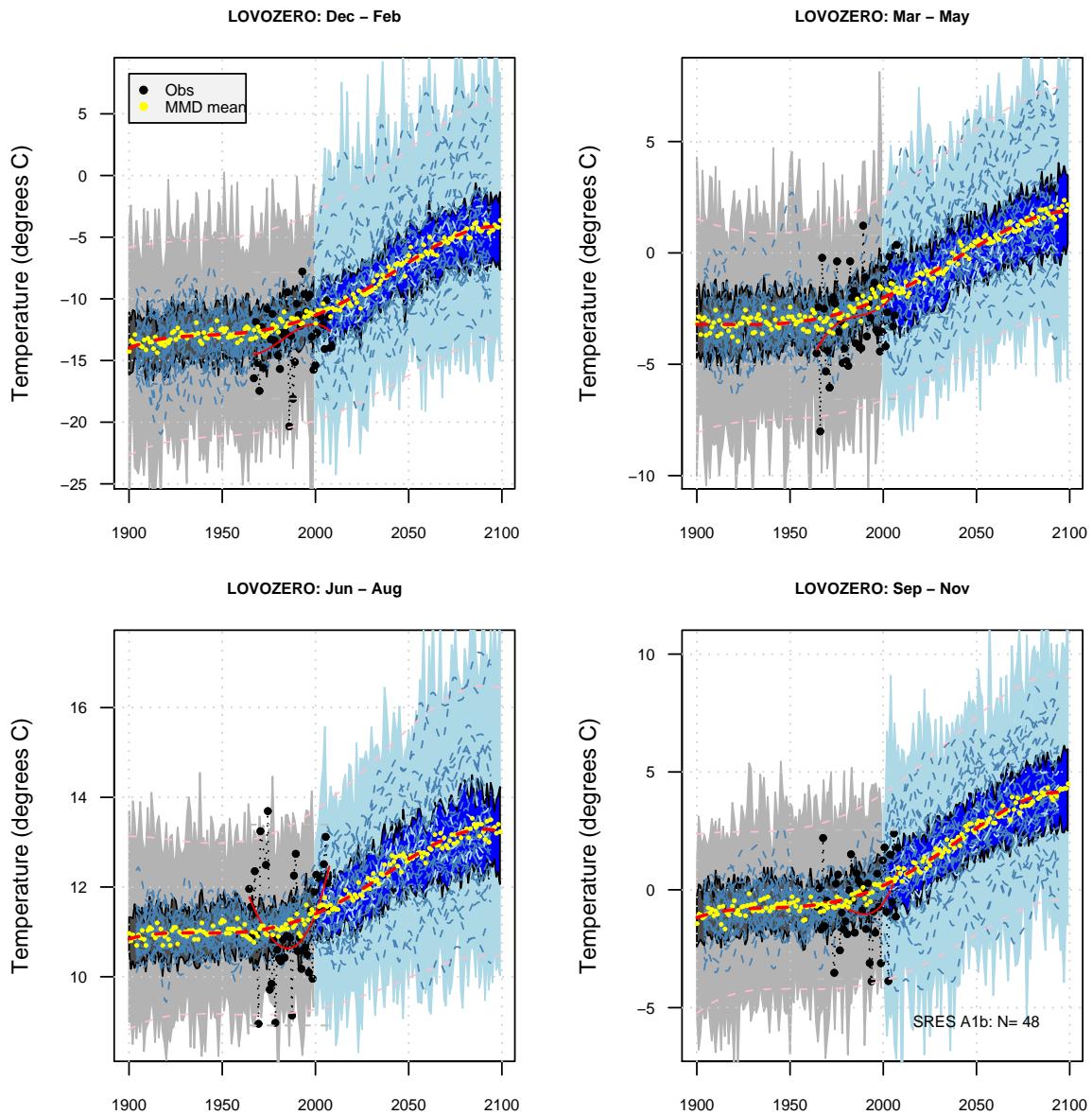
Figure 14: As in Figure 3, but for Lovozero.
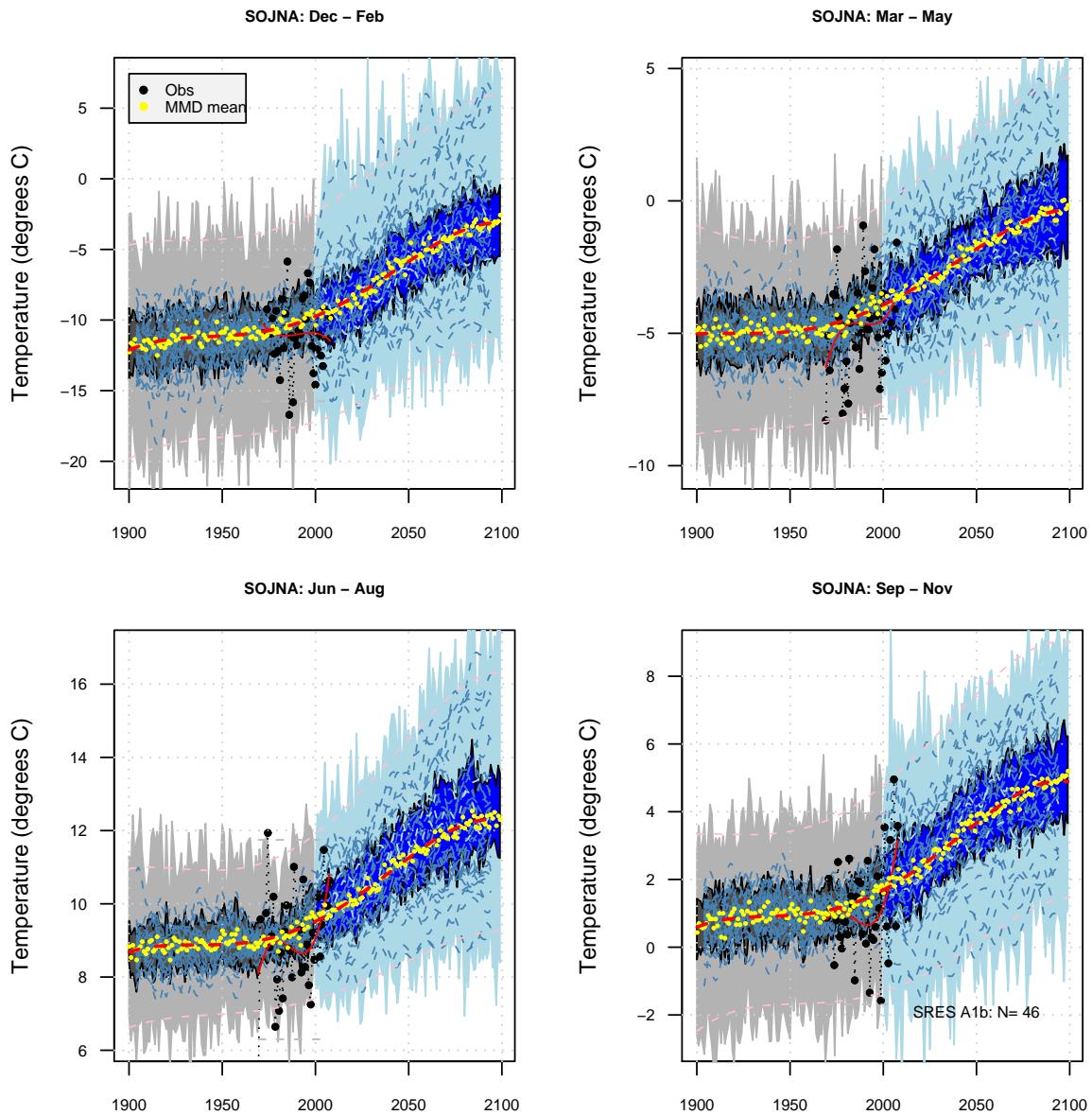
Figure 15: As in Figure 3, but for Sojna.
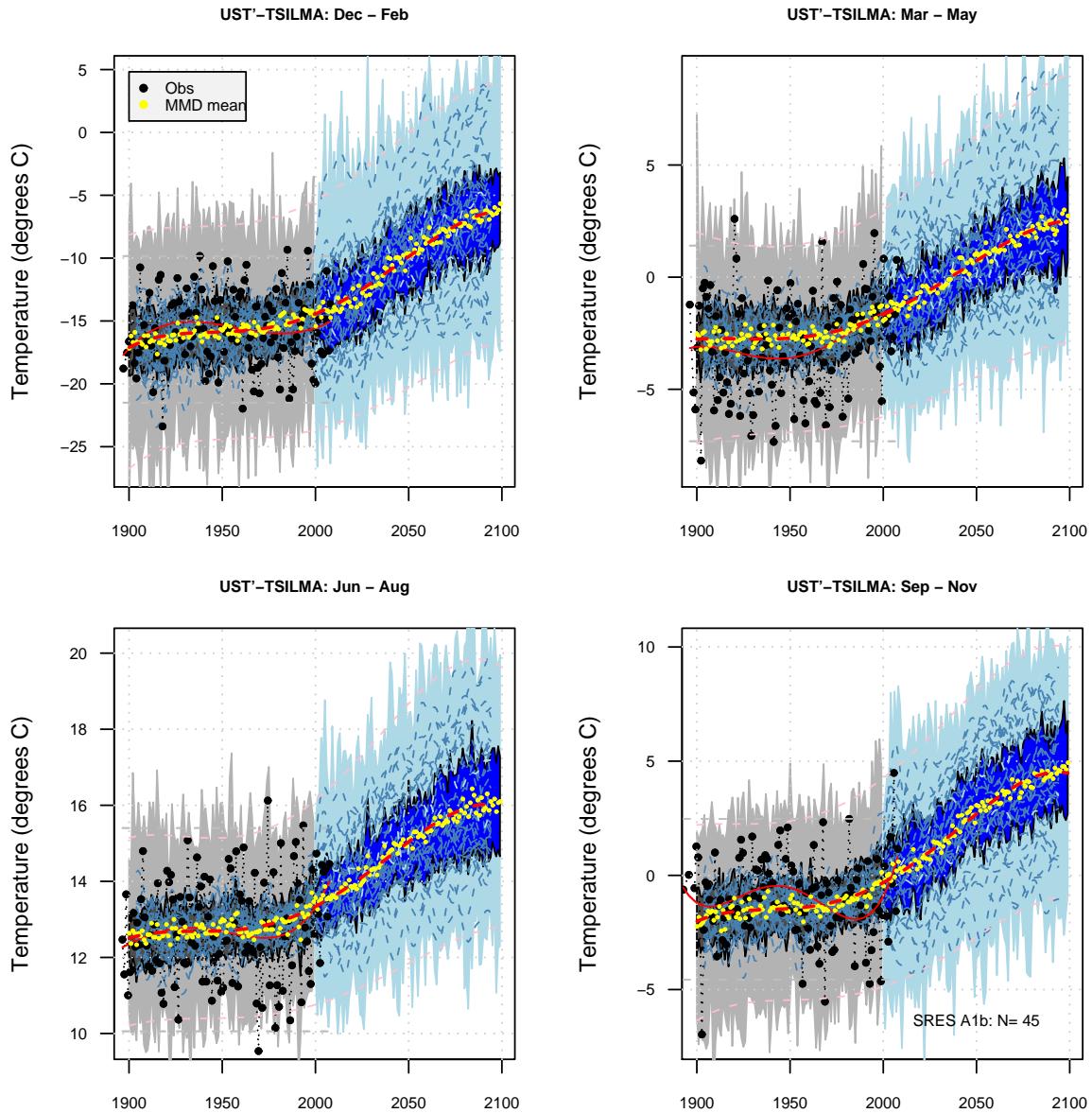
Figure 16: As in Figure 3, but for Ust'-Tsilma.
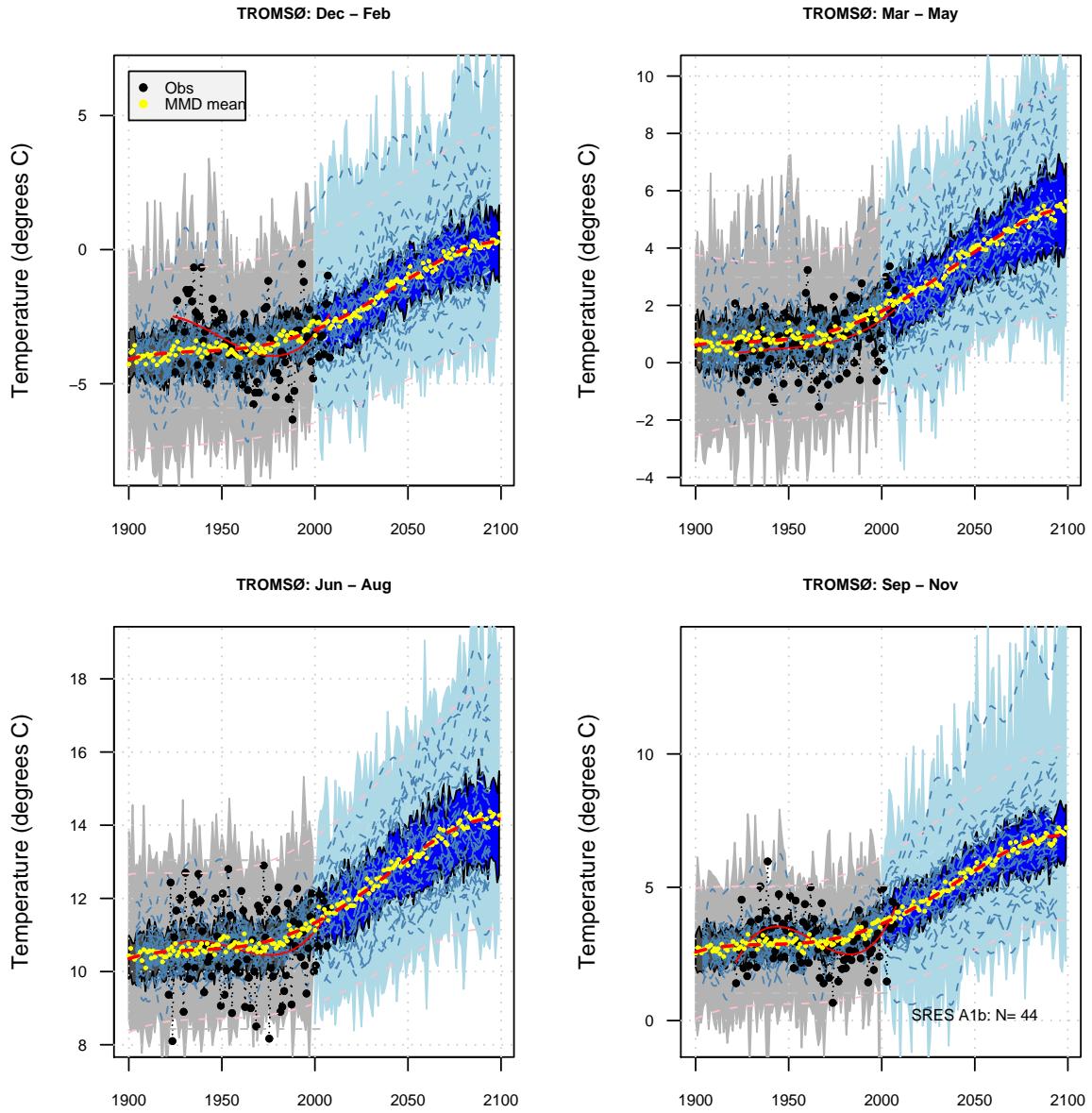
Figure 17: Plume plot for Tromsø (national code 90450; WMO code 01026). Results from the NorACIA project.
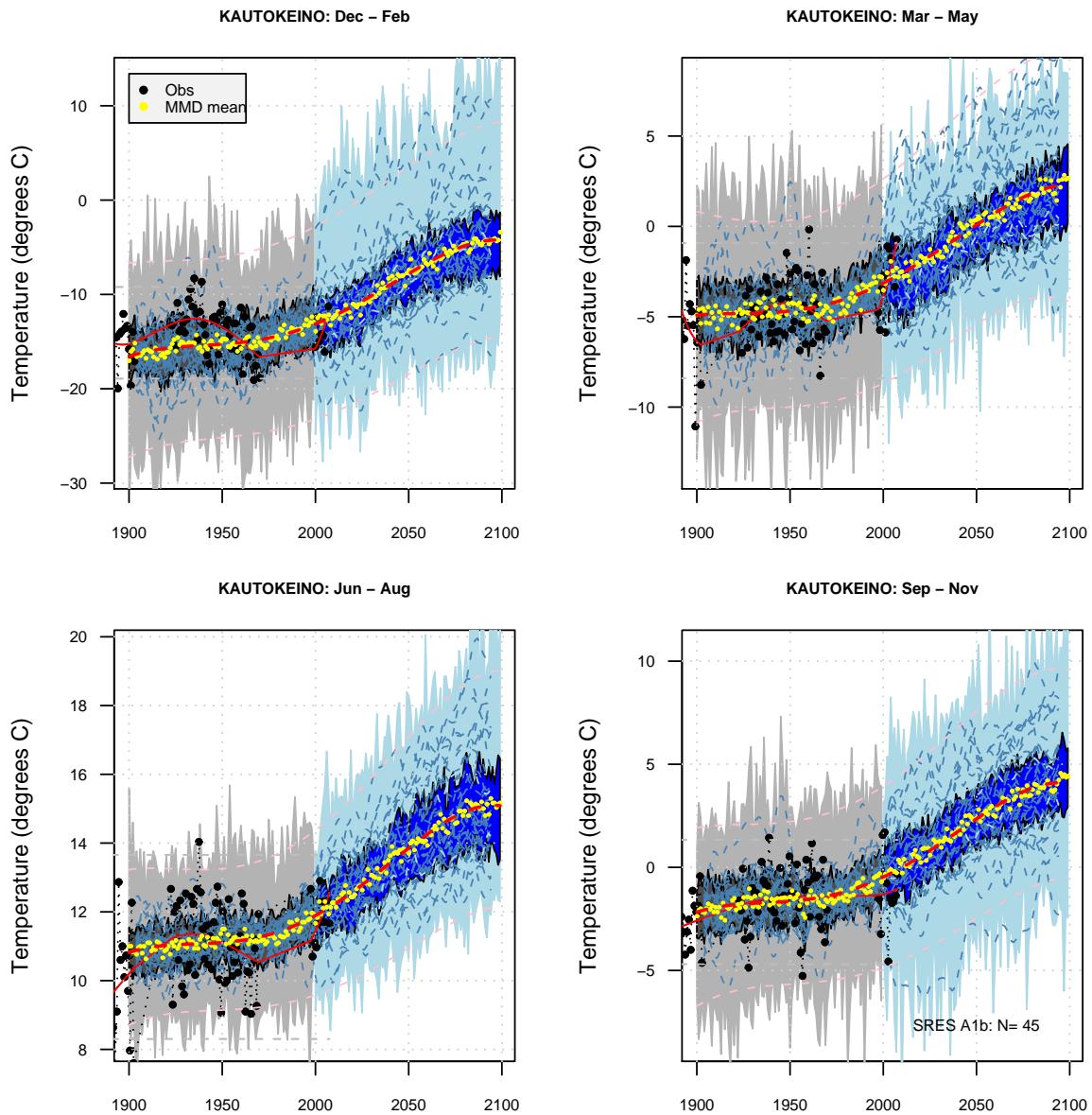
Figure 18: As in Figure 17, but for Kautokeino (national code 93700; WMO 01047).
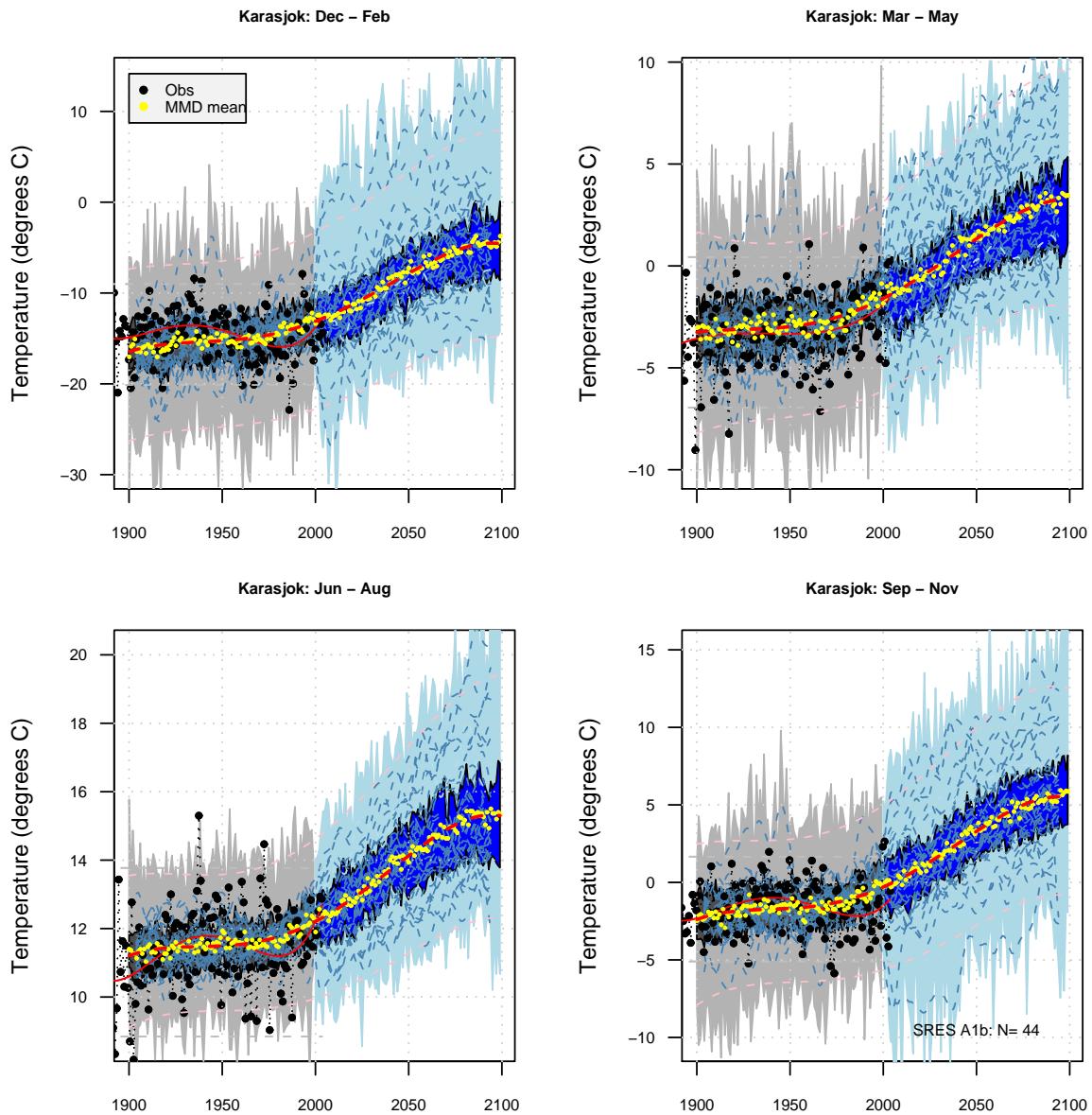
Figure 19: As in Figure 17, but for Karasjok (national code 97250; WMO 01065).
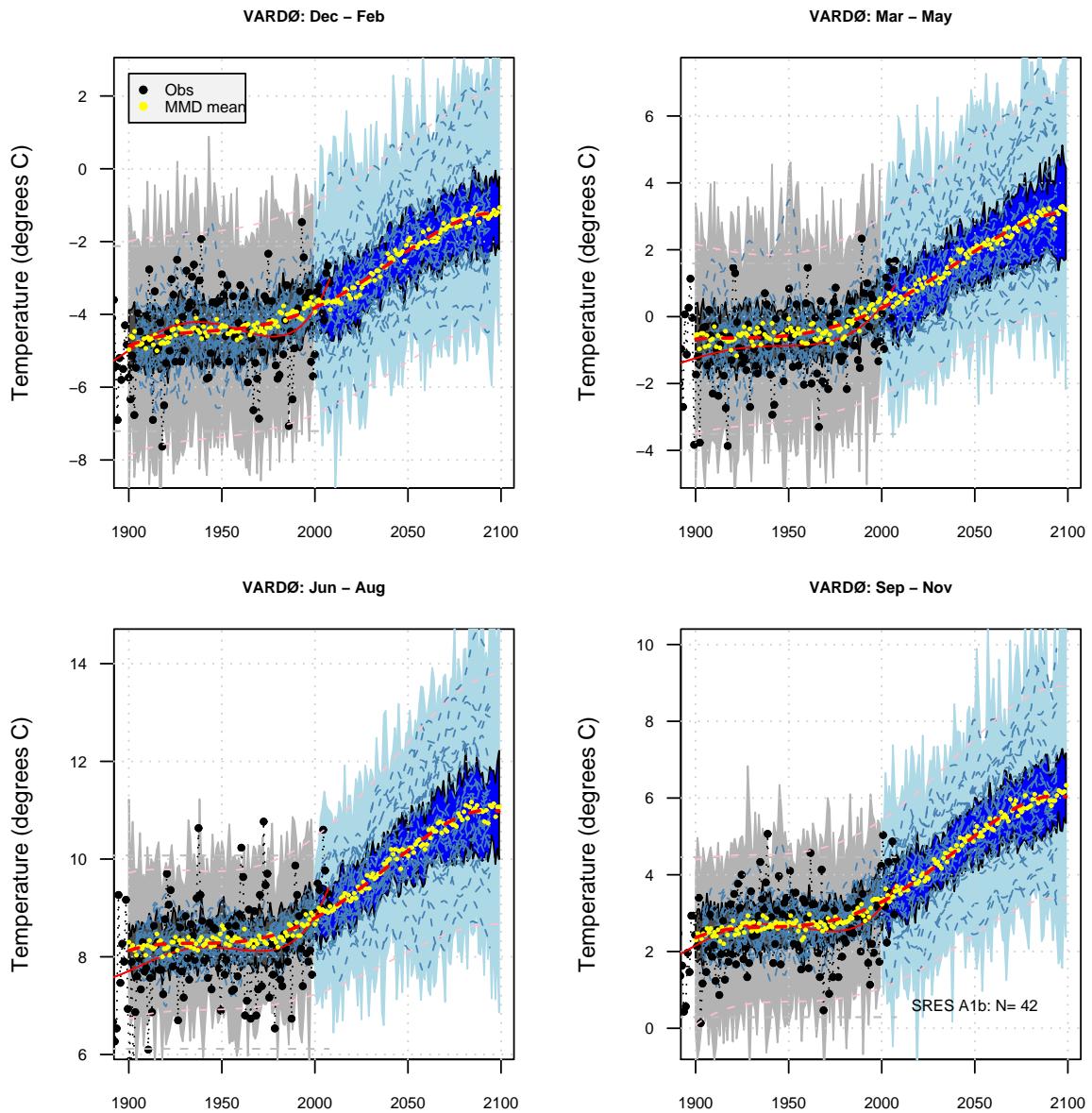
Figure 20: As in Figure 17, but for Vardø (national code 98550; WMO 01098).
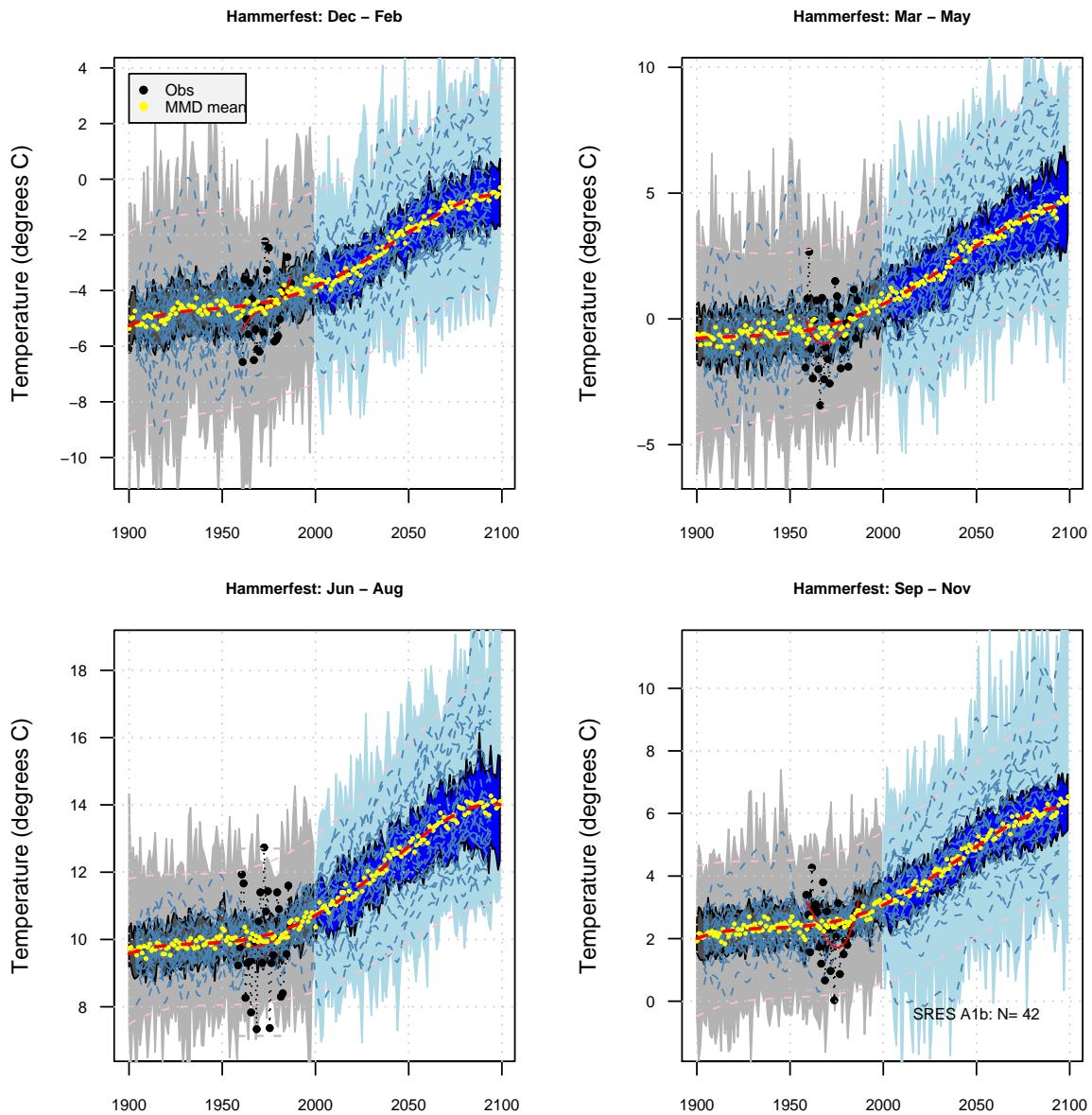
Figure 21: As in Figure 3, but for Hammerfest (national code 94260; WMO 01053).

Table 1: Seasonal mean temperature (unit: °C): mean seasonal temperature over the reference climatology ('TAM(1961–1990)'), estimated for the future 2070–2099 interval ('TAM(2070–2099)'), and the difference between these two 30-year periods ('ΔTAM(2070–2099)'). Entries shown in parentheses ('(..)') have questionable quality, and a question mark ('?') indicate that the results definitely are unreliable.

|	St. nr.	Winter	Spring	Summer	Autumn
TAM(1961–1990)					
ANADYR	25563	-20.7	-12.3	8.5	-5.9
DZALIN	21908	-36.5	-14.5	10.3	-14.5
DZHARD	24143	-36.2	-12.0	12.0	-13.1
KJUSJU	21921	-35.0	-14.1	9.8	-14.0
LOVOZE	22127	-13.5	-3.2	11.0	-0.6
OIMAKO	24688	-43.9	-14.3	11.5	-16.9
OLENEK	24125	-35.9	-12.6	11.5	-13.2
SALEKH	23330	-22.9	-8.9	11.1	-4.9
SOJNA	22271	-11.5	-4.9	8.7	0.9
TARKO-	23552	-24.0	-8.4	12.8	-5.5
TOMPO	24671	-40.6	-10.4	13.1	-14.2
UST'-T	23405	-16.1	-2.8	12.6	-1.3
YAKUTS	24959	-38.6	-7.0	16.4	-10.7
ZHIGAN	24343	-36.8	-10.9	13.2	-12.3
TROMSØ	01026	-4.0	0.8	10.5	2.7
KAUTOK	01047	-16.0	-5.2	10.7	-1.0
KARASJ	01065	-15.9	-3.2	11.3	-1.8
VARDØ	01098	-4.7	-0.7	8.2	2.6
HAMMER	01053	-4.8	-0.7	9.9	2.2
TAM(2070–2099)					
ANADYR	25563	-13.1±6.9	-7.3±4.1	12.5±3.5	0.0±4.6
DZALIN	21908	-30.4±4.3	-10.3±3.2	13.8±3.1	-7.8±4.4
DZHARD	24143	-30.3±3.6	-7.9±3.4	15.0±3.1	-6.1±4.3
KJUSJU	21921	-29.3±4.1	-11.5±3.0	12.7±3.3	-5.9±4.8
LOVOZE	22127	-5.0±6.9	1.3±4.2	13.1±2.3	3.8±3.7
OIMAKO	24688	-39.3±4.6	-11.4±2.8	14.0±2.5	-11.9±4.0
OLENEK	24125	-29.4±4.3	-8.8±3.2	14.7±3.1	-5.6±4.8
SALEKH	23330	-15.9±5.9	-3.3±4.9	14.5±3.0	0.9±4.3
SOJNA	22271	-3.9±6.4	-0.8±3.7	11.9±3.0	4.7±3.0
TARKO-	23552	-16.3±6.0	-3.1±4.7	16.4±3.0	1.7±4.7
TOMPO	24671	-35.7±3.8	-7.7±2.8	15.2±2.1	-9.6±3.2
UST'-T	23405	-7.1±8.1	1.7±4.6	15.6±2.8	4.2±4.4
YAKUTS	24959	-32.4±3.7	-3.5±2.9	19.1±2.5	-4.0±3.8
ZHIGAN	24343	-31.5±3.0	-7.3±3.0	16.1±2.9	-5.8±4.0
TROMSØ	01026	-0.1±3.0	4.9±3.4	13.8±2.8	6.7±2.7
KAUTOK	01047	-5.2±8.4	1.5±5.4	14.6±2.8	3.8±3.9
KARASJ	01065	-5.6±8.5	2.5±4.9	14.9±2.9	5.1±5.6
VARDØ	01098	-1.5±2.5	2.7±2.8	10.7±2.1	5.8±2.2
HAMMER	01053	-0.9±2.6	4.0±3.7	13.6±2.9	5.9±2.4

Table 1 continued...

ΔTAM(2070$-$2099)

ANADYR	25563	7.6±6.9	5.1±4.1	3.9±3.5	5.9±4.6
DZALIN	21908	6.0±4.3	4.2±3.2	3.4±3.1	6.8±4.4
DZHARD	24143	5.9±3.6	4.1±3.4	3.0±3.1	7.0±4.3
KJUSJU	21921	5.8±4.1	2.6±3.0	2.9±3.3	8.1±4.8
LOVOZE	22127	8.5±6.9	4.5±4.2	2.2±2.3	4.4±3.7
OIMAKO	24688	4.7±4.6	2.9±2.8	2.5±2.5	5.0±4.0
OLENEK	24125	6.5±4.3	3.7±3.2	3.2±3.1	7.5±4.8
SALEKH	23330	7.0±5.9	5.6±4.9	3.4±3.0	5.7±4.3
SOJNA	22271	7.6±6.4	4.1±3.7	3.2±3.0	3.8±3.0
TARKO-	23552	7.7±6.0	5.3±4.7	3.6±3.0	7.2±4.7
TOMPO	24671	4.9±3.8	2.7±2.8	2.1±2.1	4.6±3.2
UST'-T	23405	9.0±8.1	4.6±4.6	3.0±2.8	5.6±4.4
YAKUTS	24959	6.2±3.7	3.4±2.9	2.8±2.5	6.7±3.8
ZHIGAN	24343	5.2±3.0	3.6±3.0	2.9±2.9	6.5±4.0
TROMSØ	01026	3.8±3.0	4.2±3.4	3.3±2.8	3.9±2.7
KAUTOK	01047	10.8±8.4	6.7±5.4	3.9±2.8	4.7±3.9
KARASJ	01065	10.4±8.5	5.7±4.9	3.5±2.9	6.9±5.6
VARDØ	01098	3.3±2.5	3.4±2.8	2.6±2.1	3.3±2.2
HAMMER	01053	3.9±2.6	4.7±3.7	3.7±2.9	3.7±2.4

5   Discussion & Conclusions

Results from the CMIP3 simulations following the SRES A1b scenario were used to derive local temperature evolution for a number of sites in Russia, based on empirical-statistical downscaling (ESD) similar to the analysis published by *Benestad* (2005). The downscaled results based on projections for the future suggest an accelerated warming in the future for all seasons. A rough estimate of the seasonal mean temperature increase between 1961–90 to 2070–99 is ∼2–11°C. The ESD seems to capture much of the variance of the monthly temperature data, and the results from the downscaling itself is considered to be robust. The projected warming for the Russian sites west of 80°E is found to be strongest in winter, as in two of the Norwegian sites. For Tromsø and Vardø, the strongest estimated warming was derived for the spring season. For most of the sites in the eastern Siberia, the strongest future warming was computed to take place in during the autumn. However, the ESD results for Tompo and Anadyr suggested strongest warming in winter.

References

Anderson, D.L.T, & Carrington, D., 1994. Simulation of Tropical Variability as a Test of Climate Models. *In:* Speranza, A., & nd R. Fantechi, S.Tibaldi (eds), *Global Change*. Environment and Quality of Life, vol. EUR 15158 EN. European Commission.

Benestad, R.E., 2001. A comparison between two empirical downscaling strategies. *Int. J. Climatology*, **21**, 1645–1668. DOI 10.1002/joc.703.

Benestad, R.E., 2003a. *Downscaling analysis for daily and monthly values using clim.pact-V.0.9*. KLIMA 01/03. met.no, PO Box 43 Blindern, 0313 Oslo, Norway (www.met.no).

Benestad, R.E., 2003b. What can present climate models tell us about climate change? *Climatic Change*, **59**, 311–332.

Benestad, R.E., 2004. Empirical-Statistical Downscaling in Climate Modeling. *Eos*, **Volume 85**(42), p. 417.

Benestad, R.E., 2005. Climate change scenarios for northern Europe from multi-model IPCC AR4 climate simulations. *Geophys. Res. Lett.*, **32**(doi:10.1029/2005GL023401), L17704.

Benestad, R.E., 2008a. *Downscaled regional Norwegain temperature and precipitation series: Analysis for Statnett and CES*. Climate 7. met.no, www.met.no.

Benestad, R.E., 2008b. *Heating degree days, Cooling degree days and precipitation in Europe: Analysis for the CELECT-project*. Climate 4. met.no, www.met.no.

Benestad, R.E., Hanssen-Bauer, I., & Førland, E.J., 2007. An Evaluation of Statistical Models for Downscaling Precipitation and Their Ability to Capture Long-Term Trends. *International Journal of Climatology*, **27**(10.1002/joc.1421), 649–665.

Benestad, R.E., Chen, D., & Hanssen-Bauer, I., 2008. *Empirical-Statistical Downscaling*. Singapore: World Scientific Publishing.

Bengtsson, L., 1996. The Climate response to the Changing Greenhouse Gas Concentration in the Atmosphere. *In:* Anderson, D.L.T., & Willebrand, J. (eds), *Decadal Variability*. NATO ASI series, vol. 44. Springer.

Bengtsson, L., Hodges, K.I., & Hagemann, S., 2004. Sensitivity of the ERA40 reanalysis to the observing system: determination of the global atmospheric circulation from reduced observations. *Tellus*, **56A**, 456–471.

Christensen, J.H., & Christensen, O.B., 2002. Severe summertime flooding in Europe. *Nature*, **421**, 805.

Christensen, J.H., Räisänen, J., Iversen, T., Bjørge, D., Christensen, O. B., & Rummukainen., 2001. A synthesis of regional climate change simulations - A Scandinavian perspective. *Geophys. Res. Lett.*, **28**(6), 1003.

Christensen, J.H., Hewitson, B., Busuioc, A., A. Chen, X. Gao, Held, I., Jones, R., Kolli, R.K., Kwon, W.-T., Laprise, R., na Rueda, V. Maga Mearns, L., Menéndez, C.G., Räisänen, J., Rinke, A., Sarr, A., & Whetton, P., 2007a. *Climate Change: The Physical Science Basis*. United Kingdom and New York, NY, USA: Cambridge University Press. Chap. Regional Climate Projections.

Christensen, J.H., Hewitson, B., Busuioc, A., A. Chen, X. Gao, Held, I., Jones, R., Kolli, R.K., Kwon, W.-T., Laprise, R., na Rueda, V. Maga Mearns, L., Menéndez, C.G., Räisänen, J., Rinke, A., Sarr, A., & Whetton, P., 2007b. *Climate Change: The Physical Science Basis*. United Kingdom and New York, NY, USA: Cambridge University Press. Chap. Regional Climate Projections.

Christensen, O.B., J.H., Christensen, Machenhauer, B., & Botzet, M., 1998. Very High-Resolution Climate Simulations over Scandinavia - Present Climate. *Journal of Climate*, **11**, 3204–3229.

Crane, R.G., & Hewitson, B.C., 1998. Doubled CO_2 Precipitation Changes for the Susquehanna Basin: Downscaling from the Genesis General Circulation Model. *International Journal of Climatology*, **18**, 65–76.

Easterling, D.R., 1999. Development of regional climate scenarios using a downscaling approach. *Climatic Change*, **41**, 615–634.

Engen-Skaugen, T., Benestad, R.E., & Roald, L.A., 2007. *Empirically downscaling of runoff in Norway; Is it feasible?* Climate 15. met.no, www.met.no.

Engen-Skaugen, T., Benestad, R.E., & Førland, E.J., 2008. *Empirically downscaled precipitation and temperature representing Norwegian catchments*. Climate in progress. met.no, www.met.no.

Fleagle, R.G., & Businger, J.A., 1980. *An Introduction to Atmospheric Physics*. 2 edn. International Geophysics Series, vol. 25. Orlando: Academic Press.

Fowler, H.J., Blenkinsop, S., & Tebaldi, C., 2007. Linking climate change modelling to impacts studies: recent advances in downscaling techniques for hydrological modelling. *International Journal of Climatology*, **27**, 1547–1578.

Hanssen-Bauer, I., Achberger, C., Benestad, R.E., Chen, D., & Førland, E.J., 2005. Statistical downscaling of climate scenarios over Scandinavia: A review. *Climate Research*, **29**, 255–268.

Haugen, J.E., & Ødegaard, V., 2003. Evaluation of MPI and Hadley simulations with HIRHAM, and sensitivity to integration domains. *Pages 19–29 of:* Iversen, T., & Lystad, M. (eds), *RegClim*. General Technical report, no. 7. http://regclim.met.no/: NILU.

Haugen, J.E., Bjørge, D., & Nordeng, T.E., 2000. Dynamical downscaling PT1: Further results. *Pages 79–82 of:* Iversen, T., & Høiskar, B.A.K. (eds), *RegClim*. General Technical report, no. 4. http://www.nilu.no/regclim/: NILU.

Houghton, J.T., 1991. *The physics of atmospheres*. Cambridge, U.K.: Cambridge University Press.

Houghton, J.T., Ding, Y., Griggs, D.J., Noguer, M., van der Linden, P.J., Dai, X., Maskell, K., & Johnson, C.A., 2001. *Climate Change 2001: The Scientific Basis.* Contribution of Working Group I to the Third Assessment Report of IPCC. International Panel on Climate Change, (Available from www.ipcc.ch).

IPCC., 1990. Climate Change: The Scientific Assessment. IPCC. Cambridge University Press.

IPCC., 1995. *The Second Assessment Report*. Technical Summary. WMO & UNEP, http://www.ipcc.ch/pub/sa(E).pdf.

Meehl, G.A., Covey, C., Delworth, T., Latif, M., McAvaney, B., Mitchell, J.F.B., Stouffer, R.J., & Taylor, K.E., 2007. THE WCRP CMIP3 Multimodel Dataset: A New Era in Climate Change Research. *Bull. Amer. Meteor. Soc.*, **88**, 1383–1394.

Meehls, G.A., Stocker, T.F., W.D.idlingstein, Gaye, A.T., Gregory, J.M., Kitoh, A., Knutti, R., murphy, J.M., Noda, A., Raper, S.C.B., Watterson, I.G., Weaver, A.J., & Zhao, Z.-C., 2007. *Climate Change: The Physical Science Basis*. United Kingdom and New York, NY, USA: Cambridge University Press. Chap. Global Climate Projections.

Nakicenovic, N, J, Alcamo, G, Davis, de Vries B, J, Fenhann, S, Gaffin, K, Gregory, A, Grübler, T, Young Jung, T, Kram, EL, La Rover, L, Michaelis, Mori S, Morita T, W, Pepper, H,

Pitcher, L, Price, K, Rihai, A, Roehrl, HH, Rogner, A, Sankovski, M, Schlesinger, P, Shukla, S, Smith, R, Swart, van Rooijen S, N, Victor, & Z, Dadi (eds)., 2000. *Special report on emission scenarios. A special report of working group III of the intergovernmental Panel on Climate Change*. Cambridge University Press, Cambridge. Chap. 4.

Peixoto, J.P., & Oort, A.H., 1992. *Physics of Climate*. N.Y.: AIP.

Philander, S.G., 1989. *El Niño, La Niña, and the Southern Oscillation.* N.Y.: Academic Press.

R Development Core Team., 2004. *R: A language and environment for statistical computing*. R Foundation for Statistical Computing, Vienna, Austria. ISBN 3-900051-07-0.

Robinson, P.J., & Finkelstein, P.L., 1991. The development of impact-oriented scenarios. *Bull. Am. Met. Soc.*, **4**, 481–490.

Rummukainen, M., 1997. *Methods for Statistical downscaling of GCM simulations*. SWE-CLIM 80. SMHI.

Sarachik, E.S., Winton, M., & Yin, F.L., 1996. Mechanisms for Decadal-to-Centennial Climate Variability. *In:* Anderson, D.L.T., & Willebrand, J. (eds), *Decadal Variability*. NATO ASI series, vol. 44. Springer.

Simmons, A.J., & Gibson, J.K., 2000. *The ERA-40 Project Plan.* ERA-40 Project Report Series 1. ECMWF, www.ecmwf.int.

Solomon, S., Quin, D., Manning, M., Chen, Z., Marquis, M., Averyt, K.B., Tignotr, M., & Miller, H.L. (eds)., 2007. *Climate Change: The Physical Science Basis. Contribution of Working Gropu I to the Fourth Assessment Report of the Intergovernmental Panel on Climate Change*. United Kingdom and New York, NY, USA: Cambridge University Press.

Treut, H. Le., 1994. Cloud Representation in Large-Scale Models: Can we Adequately Constrain them through Observed Data? *In:* Speranza, A., & nd R. Fantechi, S.Tibaldi (eds), *Global Change*. Environment and Quality of Life, vol. EUR 15158 EN. European Commission.

von Storch, H., Zorita, E., & Cubasch, U., 1993a. Downscaling of Global Climate Change Estimates to Regional Scales: An Application to Iberian Rainfall in Wintertime. *Journal of Climate*, **6**, 1161–1171.

von Storch, H., Zorita, E., & Cubasch, U., 1993b. Downscaling of Global Climate Change Estimates to Regional Scales: An Application to Iberian Rainfall in Wintertime. *Journal of Climate*, **6**, 1161–1171.

Weart, S., 2003. *Discovery of Global Warming*. Harvard University Press.

Wilby, R.L., Hassan, H., & Hanaki, K., 1998. Statistical downscaling of hydrometeorological variables using general circulation model output. *Journal of Hydrology*, **205**, 1–19.

Wilby, R.L., Charles, S.P., Zortia, E., Timbal, B., Whetton, P., & Mearns, L.O., 2004. *Guidelines for Use of Climate Scenarios Developed from Statistical Downscaling Methods*. Supporting material of the Intergovernmental Panel on Climate Change. Task group on Data and Scenario Support for Impacts and Climate Analysis.

Zorita, E., & von Storch, H., 1997. *A survey of statistical downscaling results*. Tech. rept. 97/E/20. GKSS.

Appendix

Box-plots for temperature

The box-plot diagrams shown here correspond to the lower panels in Figures 3–8.
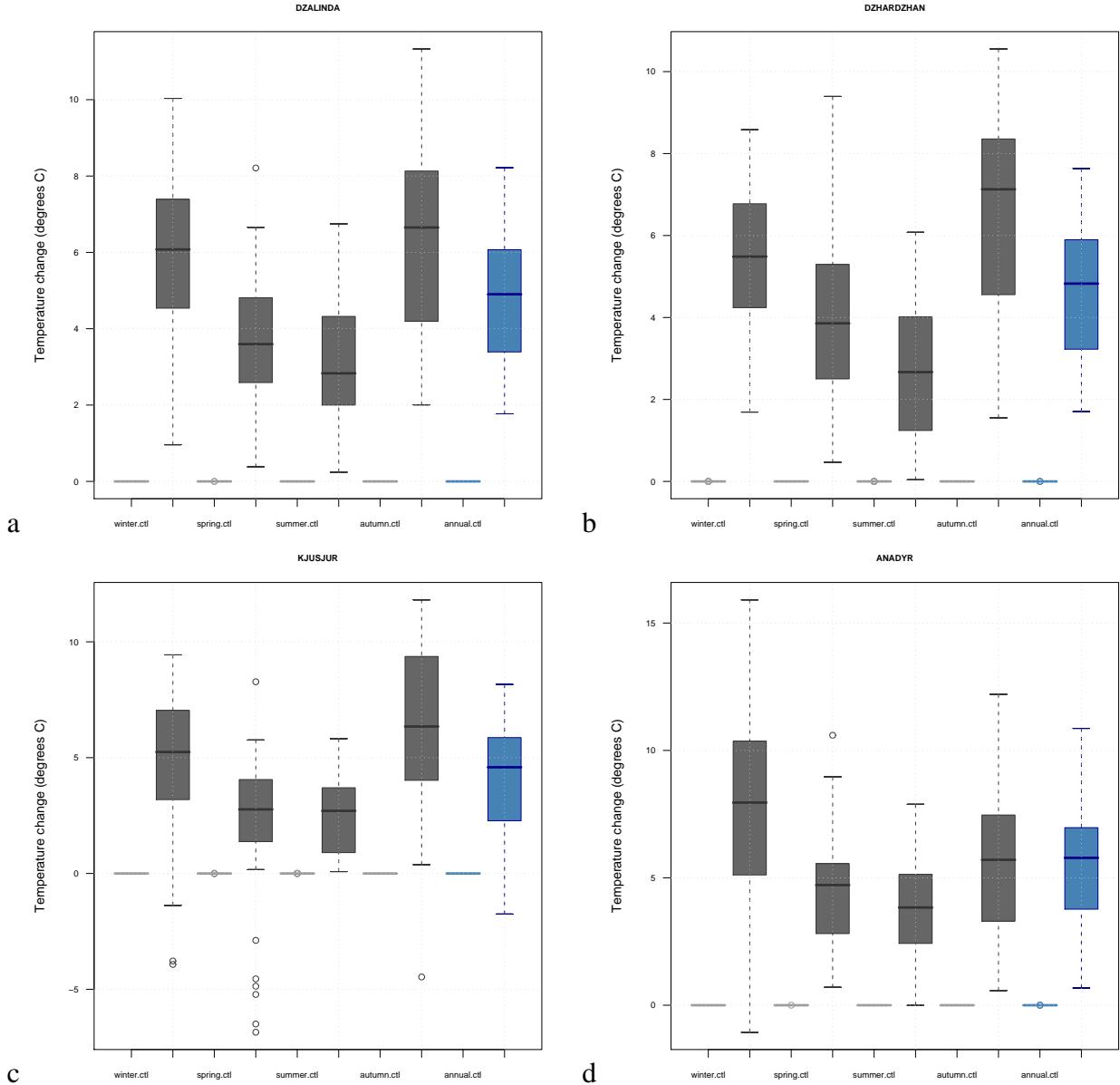
Figure 22: Box-plots showing estimated seasonal and annual mean change from 1961–1990 (CTL; the 20th Century runs) to 2070–2099 (SRES A1b). Light grey boxes show the spread of the 1961–1990 CTL around the mean value and dark boxes show the change from the 1961–1990 period. Blue boxes show the annual mean values. Each box shows the ensemble inter-quantile range (IQR: 25%–75%), and the horizontal lines within mark the ensemble median. The whiskers extend $1.5\times$ IQR from the box boundary, and data points beyond this range are regarded as outliers (circular symbols).

40
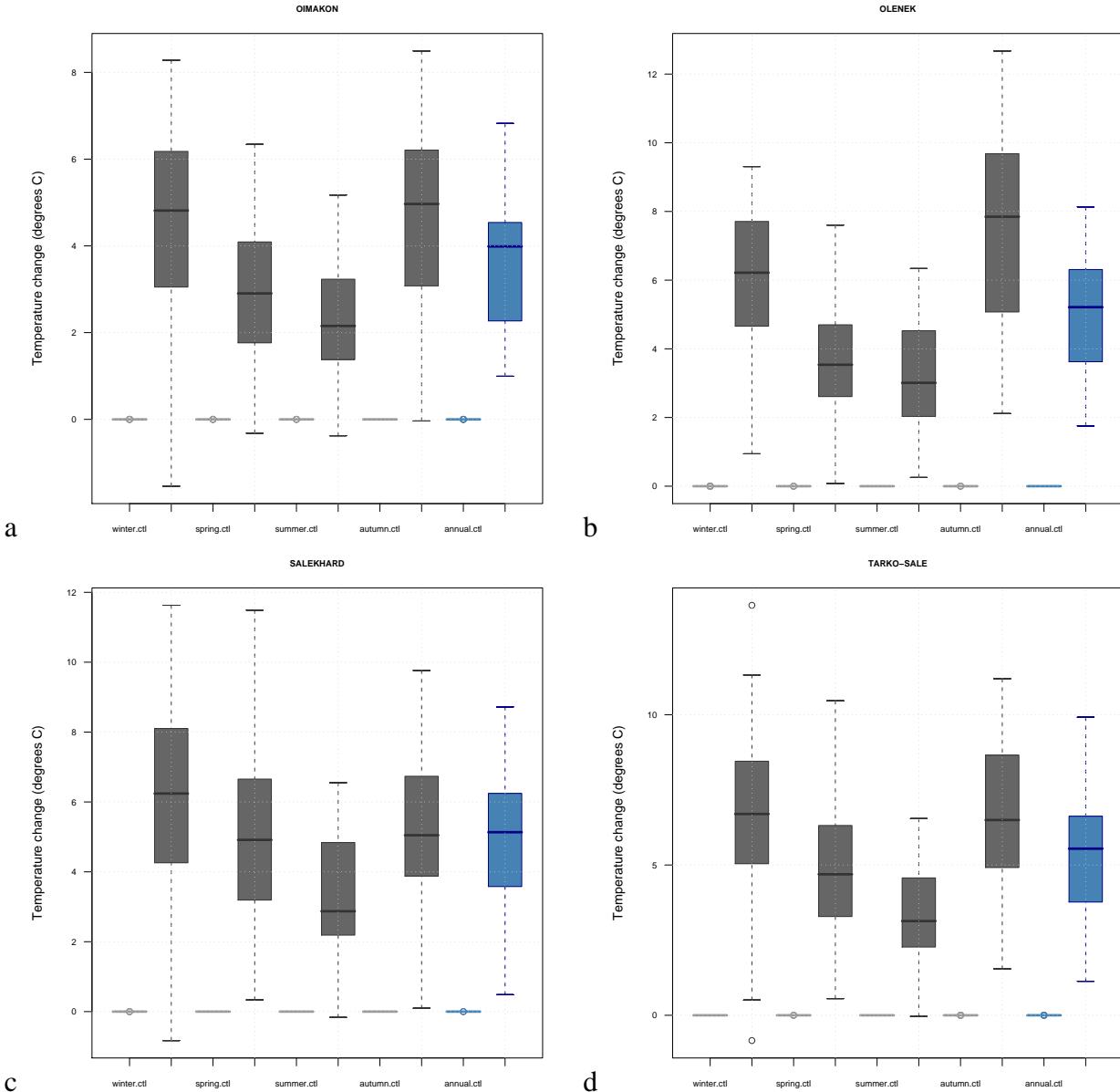
Figure 23: Same as Figure 22.

41
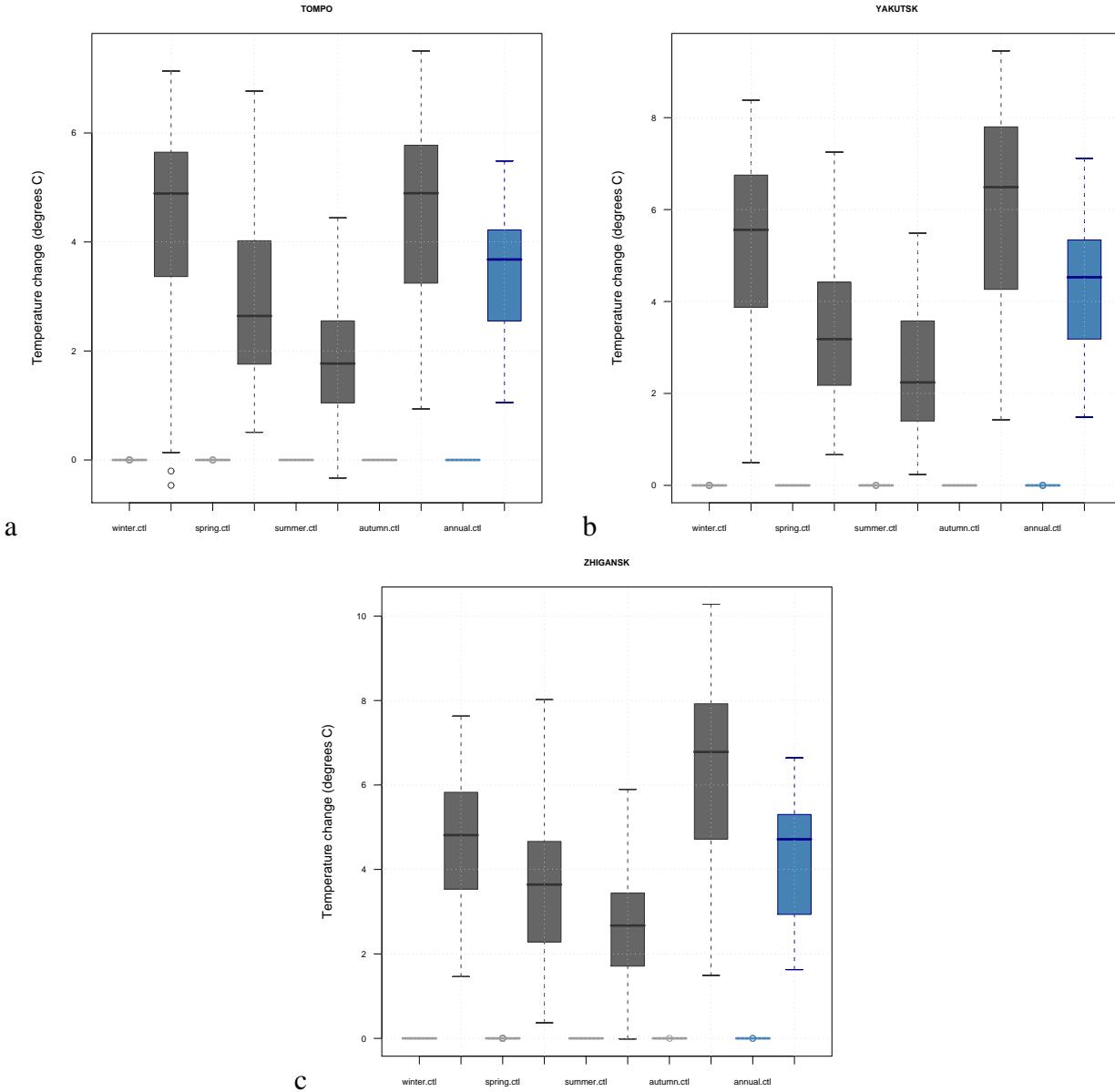
Figure 24: Same as Figure 22.

Quality evaluation of downscaling of temperature

In order to get a feeling for uncertainties involved in the ESD, the R^2-statstics from the regression analysis was checked for two arbitrary selected regions. Figure 25 show how the R^2-statistics varies between GCMs (left) and the calendar month (right) for temperature regions 1 and 2. These results verify the impression from Figures 3–8 which show corresponding variance in the observations and the downscaled results (indicative of a high R^2-score).

Because the various GCMs may differ in their ability to provide an exact representation of the spatio-temporal structure of the temperature modes, the common EOFs may differ somewhat from GCM to GCM. Thus the R^2-statistics may vary with the GCM, although the variation in the R^2-statistics should be small for realistic GCMs (large deviations in the R^2-statistics may be an indicator of model problems).

Additional quality control ensuring smooth variation in the trend estimates throughout the year was not used here (*Benestad*, 2004), but the change in the trend characteristics through the year can then be used to assess the quality of the results. In other words, Figure 25–26 suggest that the results for Yakutsk is of high quality.

a

b

c

d
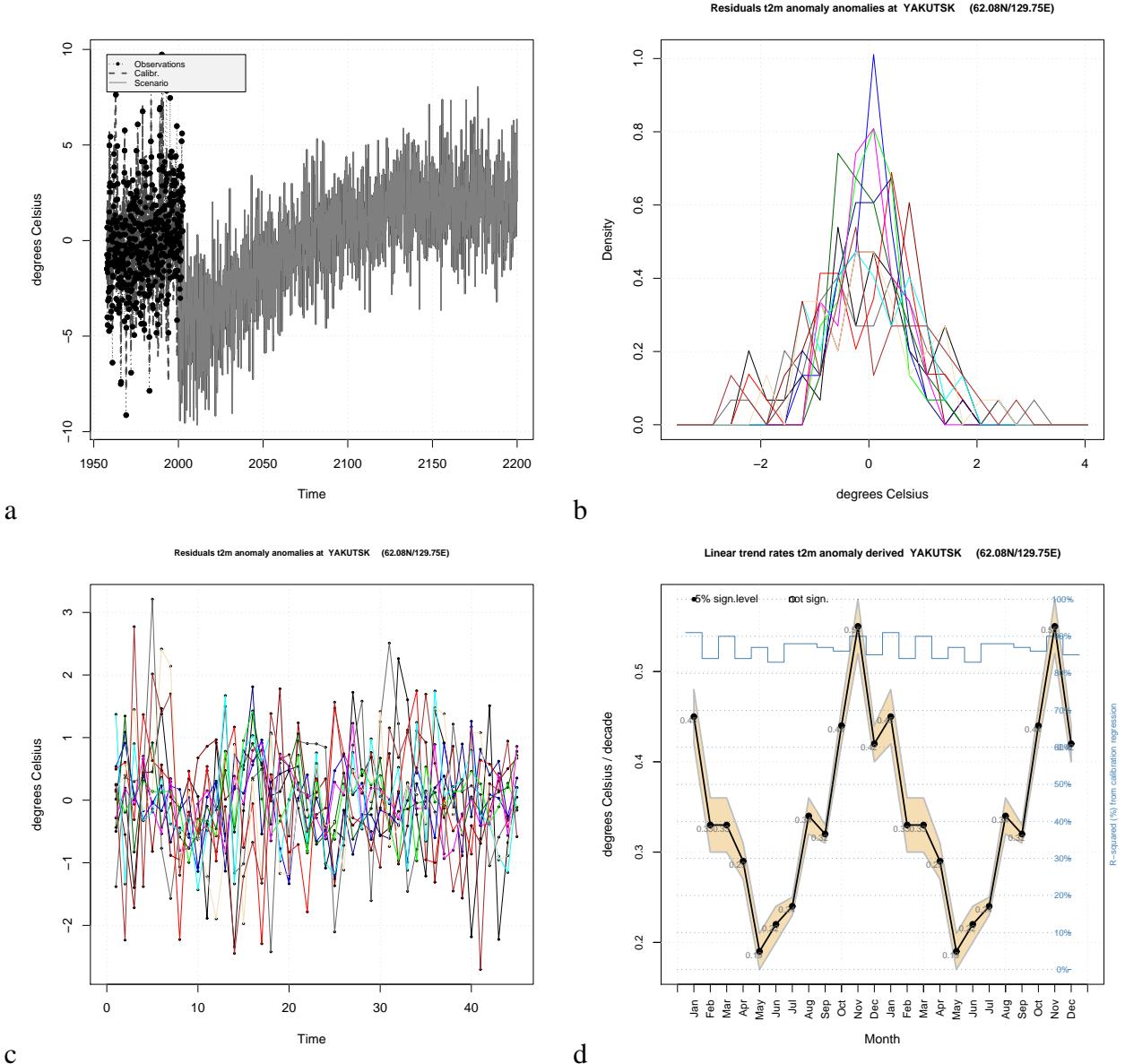
Figure 25: Diagnostics from the downscaling at Yakutsk for the whole year: (a) the downscaled time series, (b) distribution of residuals, (c) the residual time structure, and (d) the variation of trend estimates over the year. The blue curve in panel d shows the R^2 statistics from the regression, indicating values greater than 80% for all months.
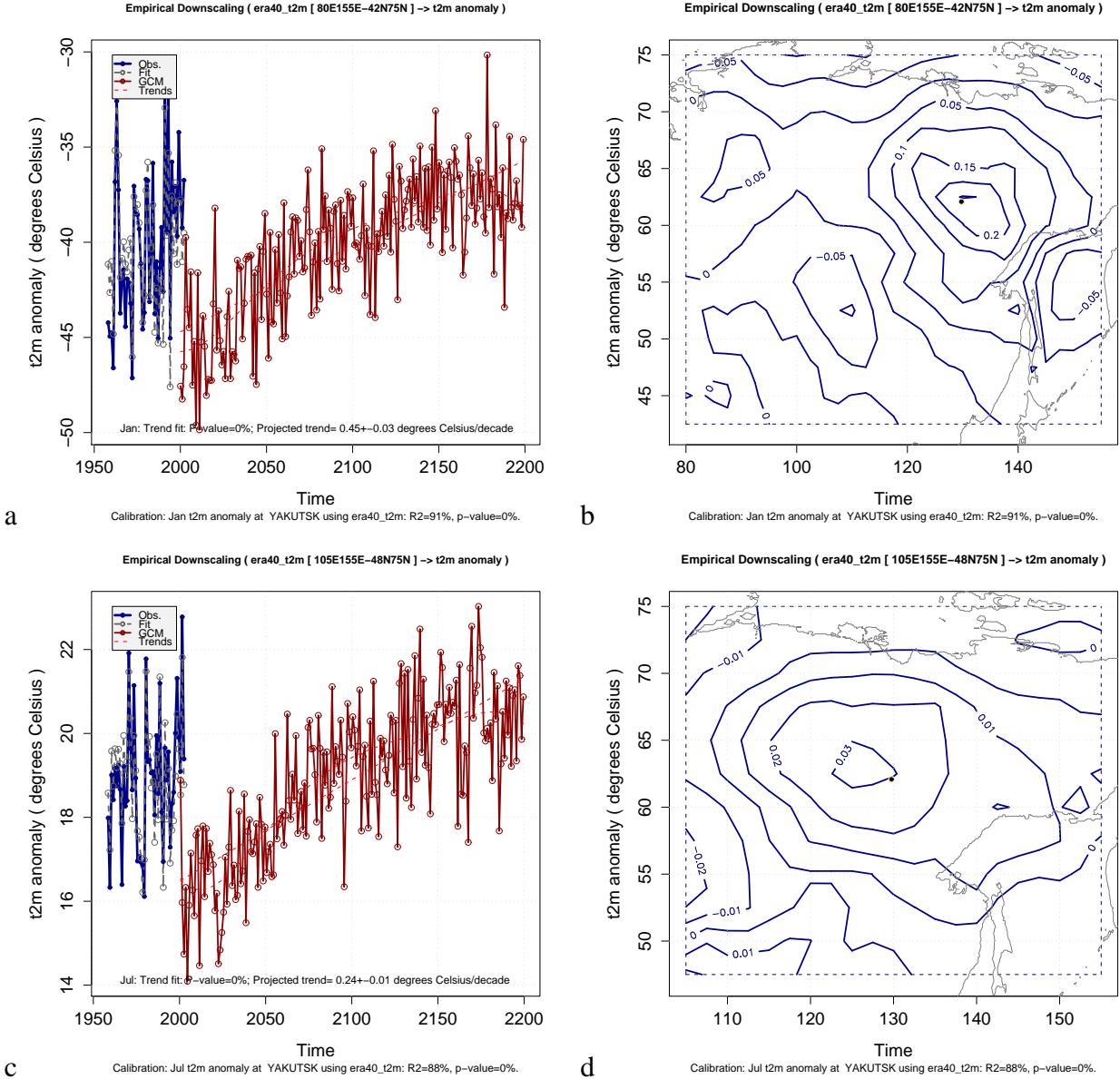
Figure 26: Diagnostics from the downscaling of January and July months at Yakutsk.

Table 2: List of the GCMs and the scenario simulations used as input for the ESD-based scenario production. The choice of runs was arbitrary in the sense that only those results that were available at the time of the downloading were selected. The GCMs iap_fgoals1_0_g and cccma_cgcm3_1 were excluded from the present analysis, due to questionable results.

Temperature:

GCM	SRES A1b	c20
bcc_cm1		run 1–2
bccr_bcm2_0	run 1	run 1
cnrm_cm3	run 1	run 1
csiro_mk3_0		run 1
gfdl_cm2_0	run 1	run 1
gfdl_cm2_1	run 1	run 1–3
giss_aom	run 1–2	run 2
giss_model_e_h	run 1–3	run 1–5
giss_model_e_r	run 1–5	
inmcm3_0	run 1	run 1
ipsl_cm4	run 1	run 1
miroc3_2_hires	run 1	
miroc3_2_medres	run 2,3	
miub_echo_g	run 1,3	
mpi_echam5	run 1–3	run 1–3
mri_cgcm2_3_2a	run 1–5	
ncar_ccsm3_0	run 1,2,3	run 1,3,6,9
ncar_pcm1	run 1–3	run 2,3,4
ukmo_hadcm3	run1	run 1,2
ukmo_hadgem1	run1	

List of GCMs

Meta data

LIST OF STATIONS

WMO		Latitude	Longitude	Elevation	Name	Date_started	Region
22127		68.05	34.80	161	Loveozero	1936	Kola_peninsula
22271		67.88	44.13	8	Soina	1936	Nenets_AA
23405		65.43	52.17	68	Ust'-Tsilma	1889	Republic_Komi
23552		64.92	77.82	27	Tarko-Sale	1936	Iamalo-Nenets_AA
23242		67.42	72.54	12	Novyi-Port	1924	Iamalo-Nenets_AA
23330		66.32	66.32	NA	Salekhard	1883	Iamalo-Nenets_AA
21921		70.41	127.24	33	Kjusjur	1888	Republic_Sakha
21921		70.41	127.24	33	Kusur	1888	Republic_Sakha
24343		66.46	123.24	92	Zhigansk	1935	Republic_Sakha
24143		68.44	124.00	39	Dzhardzhan	1936	Republic_Sakha
21908		70.08	113.58	62	Dzalinda	1947	Republic_Sakha
24382		66.27	143.14	196	Ust-Mona	1937	Republic_Sakha
25400		65.44	150.54	43	Zyrianka	1935	Republic_Sakha
25325		66.33	159.25	127	Ust-Oloi	1936	Chukchi_AA
25551		64.41	170.25	26	Markovo	1894	Chukchi_AA
25563		64.47	177.34	61	Anadyr	1895	Chukchi_AA
01065		69.46	25.50	131	Karasjok	1877	Finnmark_Norway
24125		68.50	112.43	220	Olenek	1936	Republic_Sakha?
24688		63.26	143.15	726	Oimakon	1952	Republic_Sakha?
24671		63.95	135.87	400	Tompo	1960	Republic_Sakha?
24959		62.08	129.75	101	Yakutsk	1958	Republic_Sakha?
01047	(93700)	69.00	23.03	307	Kautokeino	1889	Finnmark_Norway
01098	(98550)	70.37	31.08	14	Vardø	1829	Finnmark_Norway
01026	(90450)	69.65	18.93	100	Tromsø	1920	Troms_Norway
01053	(94260)	70.68	23.67	69	Hammerfest	1957	Finnmark_Norway
01065	(93700)	69,00	23.03	307	Karasjok	1889	Finnmark_Norway

R-script

Listing of the R-script used to derive these results (file name is dsEALAT.R):

```
rm(list=ls())
source("ds_one.R")
source("met.no/R/ESD.results.R")

s2n <- function(t) {
  spc <- instring(" ",t)
  n1 <- strip(t)
  n2 <- substr(t,spc[length(spc)]+1,nchar(t))
  c(as.numeric(n1),as.numeric(n2))
}

read.ealat <- function(name,verbose=TRUE,param="TAM") {
  header <- readLines(name,n=5)
  location <- substr(header[1],6,nchar(header[1]))
  colon <- instring(":",header[4])
  lon.deg.min <- as.numeric(s2n(substr(header[4],colon[1]+1,nchar(header[4]))))
  lon <- lon.deg.min[1]+lon.deg.min[2]/60
  colon <- instring(":",header[3])
  lat.deg.min <- as.numeric(s2n(substr(header[3],colon[1]+1,nchar(header[3]))))
  lat <- lat.deg.min[1]+lat.deg.min[2]/60
  colon <- instring(":",header[5])
  alt <- as.numeric(substr(header[5],colon[1]+1,nchar(header[5])))
  colon <- instring(":",header[2])
  wmo <- as.numeric(substr(header[2],colon[1]+1,nchar(header[2])))
  col.names=switch(param,"TAM"=c("number","year","month","day","TAM","TAX","hourflag.TAX","TAN","hourflag.TAN"),
                          "SND"=c("year","month","day","SND"))
  t2m <- read.fwf(name,widths=c(5,6,3,3,6,6,1,5,1),skip=17,col.names=col.names)
  nt <- length(t2m$year)

  if (param=="TAM") {
    t2m$TAM <- as.numeric(t2m$TAM); t2m$TAX <- as.numeric(t2m$TAX); t2m$TAN <- as.numeric(t2m$TAN)
    t2m$TAM[abs(t2m$TAM)>100] <- NA
    t2m$TAX[abs(t2m$TAX)>100] <- NA
    t2m$TAN[abs(t2m$TAN)>100] <- NA
    tam <- station.obj.dm(t2m=t2m$TAM,precip=rep(NA,nt),dd=t2m$day,mm=t2m$month,yy=t2m$year,
                          obs.name=c("mean 2-meter air temperature",NA),unit=c("degrees Celsius",NA),
                          ele=c(101,NA),station=wmo,lat=lat,lon=lon,alt=alt,
                          location=location,wmo.no=wmo,
                          start=NULL,yy0=NULL,country="Russia",
                          ref="EALAT; private communication Pavel (svyashchennikov@mail.ru)")
    tax <- station.obj.dm(t2m=t2m$TAX,precip=rep(NA,nt),dd=t2m$day,mm=t2m$month,yy=t2m$year,
                          obs.name=c("maximum air temperature",NA),unit=c("degrees Celsius",NA),
                          ele=c(101,NA),station=wmo,lat=lat,lon=lon,alt=alt,
                          location=location,wmo.no=wmo,
                          start=NULL,yy0=NULL,country="Russia",
                          ref="EALAT; private communication Pavel (svyashchennikov@mail.ru)")
    tan <- station.obj.dm(t2m=t2m$TAN,precip=rep(NA,nt),dd=t2m$day,mm=t2m$month,yy=t2m$year,
                          obs.name=c("minimum air temperature",NA),unit=c("degrees Celsius",NA),
                          ele=c(101,NA),station=wmo,lat=lat,lon=lon,alt=alt,
                          location=location,wmo.no=wmo,
                          start=NULL,yy0=NULL,country="Russia",
                          ref="EALAT; private communication Pavel (svyashchennikov@mail.ru)")
    obs.dm <- switch(as.character(param),"TAM"=tam,"TAX"=tax,"TAN"=tan)
    obs <- daily2monthly.station(obs.dm)

  } else if (param=="SND") {
    t2m$SND <- as.numeric(t2m$SND)
    snd <- station.obj.dm(t2m=t2m$SND,precip=rep(NA,nt),dd=t2m$day,mm=t2m$month,yy=t2m$year,
                          obs.name=c("Daily snow depth measured in centimeters",NA),unit=c("cm",NA),
                          ele=c(101,NA),station=wmo,lat=lat,lon=lon,alt=alt,
                          location=location,wmo.no=wmo,
                          start=NULL,yy0=NULL,country="Russia",
                          ref="Anders Oskal")
    obs <- daily2monthly.station(snd)
  }
  if (verbose) print(summary(t2m))
```

```
    invisible(obs)
}

computeEALAT <- function(param="TAM",start=1,last=NULL,LINPACK=FALSE) {
  ele <- switch(param,"TAM"=101,"RR"=601,SND=601)
  pattern <- switch(param,"TAM"="T.txt","SND"="-S.txt")
  a<-list.files("/klimadata/rasmusb/EALAT_Russland",pattern=pattern,full.names=TRUE)
  if (is.null(last)) last <- length(a)

  for (i in start:last) {
    print(a[i])
    ealat.data <- read.ealat(a[i],param=param)
    if (param=="TAM") {
      #TAM <- daily2monthly.station(ealat.data$tam)
      TAM <- ealat.data
      TAMA <- anomaly.station(TAM)
      TAM$val[abs(TAMA$val)>10] <- NA
      #TAX <- daily2monthly.station(ealat.data$tax)
      #TAX$val[abs(TAMA$val)>10] <- NA
      #TAN <- daily2monthly.station(ealat.data$tan)
      #TAN$val[abs(TAMA$val)>10] <- NA

      if ( (sum(is.element(TAM$yy,1950:2000))> 20) & (sum(is.finite(TAM$val))> 20*12) ) {
        print(paste("Downscaling",a$location))
        ds.one(ele=ele,cmons=1:12,silent=TRUE,do.a1b=TRUE,do.rcm=0,
           qc=FALSE,station=TAM,predictand="ealat.tam",op.path="/klimadata/rasmusb/EALAT",
           lon=TAM$lon+c(-20,20),lat=TAM$lat+c(-15,5),LINPACK=LINPACK)
      #  ds.one(ele=ele,cmons=1:12,silent=TRUE,do.a1b=TRUE,do.rcm=0,
      #      qc=FALSE,station=TAX,predictand="ealat.tax",op.path="/klimadata/rasmusb/EALAT",
      #      lon=TAX$lon+c(-50,50),lat=TAX$lat+c(-30,20),LINPACK=LINPACK)
      #  ds.one(ele=ele,cmons=1:12,silent=TRUE,do.a1b=TRUE,do.rcm=0,
      #      qc=FALSE,station=TAN,predictand="ealat.tan",op.path="/klimadata/rasmusb/EALAT",
      #      lon=TAN$lon+c(-50,50),lat=TAN$lat+c(-30,20),LINPACK=LINPACK)
      }
    } else if (param=="SND") {
      SND <- daily2monthly.station(ealat.data)
      d <- dim(SND$val)
      snd <- c(t(SND$val)); SND.1 <- snd[1]; snd <- c(NA,diff(snd))
      SND$val <- t(as.matrix(snd,d[2],d[1]))
      ds.one(ele=ele,cmons=1:12,silent=TRUE,do.a1b=TRUE,do.rcm=0,
            qc=FALSE,station=SND,predictand="ealat.snd",op.path="/klimadata/rasmusb/EALAT")
    }
    while (dev.cur()>1) dev.off()
  #remove.Rdata.files(path="output")
  }
}


Figures <- function(path="/klimadata/rasmusb/EALAT/",pattern="ealat.tam",minus=8,start=1) {
  ealat.meta <- read.table("EALAT-list.txt",header=TRUE)
  ele <- switch(pattern,"ealat.tam"=101,"ealat.tax"=112,"ealat.tan" = 122)
  param <- switch(pattern,"ealat.tam"="TAM","ealat.tax"="TAX","ealat.tan" = "TAN")
  a<-list.files("/klimadata/rasmusb/EALAT_Russland",pattern="T.txt",full.names=TRUE)
  locations <- list.files(path=path,pattern=pattern)
  n <- length(locations)
  locs <- rep("NA",n)
  #print(lower.case(substr(locations,10,14))); print(lower.case(substr(as.character(ealat.meta$Name),1,5)))
  for (ireg in start:n) {
    ii <- grep(lower.case(substr(locations[ireg],10,14)),lower.case(substr(as.character(ealat.meta$Name),1,5)))
    print(as.character(ealat.meta$Name[ii]))
    iii <- grep(ealat.meta$WMO[ii],a)
    locs[ireg] <- substr(locations[ireg],10,nchar(locations[ireg])-minus)
    obs.get <- paste("read.ealat('",a[iii],"',verbose=FALSE,param='",param,"')",sep="")
    print(obs.get)
    # The weeding removes all data at Tarko-Sale - switch off weeding for this location...
    if (ireg==10) {rm.bad.start <- FALSE; remove.bad.sd <- FALSE } else
                  {rm.bad.start <- TRUE; remove.bad.sd <- TRUE}

    esd <- finalPlot(path=path,predictand="ealat.tam",station=locs[ireg],ele=ele,obs.get=obs.get,
              remove.bad.sd=remove.bad.sd,rm.bad.start=rm.bad.start)
```

```
    par(cex.axis=1,las=1,mfrow=c(1,1),cex.axis=0.7,mar=c(2, 4, 3, 2) + 0.1,cex.main=0.7)
    esd$station <- substr(esd$station,nchar(pattern)+1,nchar(esd$station))
    plotESD.box(esd)
    dev.copy2eps(file=paste("Fig","_",locs[ireg],"-boxplot.eps",sep=""))
  }
}


sjekkEALAT <- function() {
  subdirs <- list.files(path="/klimadata/rasmusb/EALAT",full.names=TRUE)
  for (i in 1:length(subdirs)) {
    files <- list.files(path=subdirs[i],pattern=".Rdata",full.names=TRUE)
#    for (ii in 1:length(files)) {
      ii <- 1
      print(files[ii])
      load(files[ii])
      plotStation(x)
      action <- readline("OK?")
      plotDS(ds.station$Jan)
      action <- readline("OK?")
      plotOBJds(ds.station)
      action <- readline("OK?")
      if (lower.case(action)=="no") bad <- c(bad,subdirs)
#    }
  }
}

kart <- function(path="/klimadata/rasmusb/EALAT_Russland",pattern="T.txt") {
    data(addland2)
    lat.cont[lat.cont < 0] <- NA
    locations <- list.files(path=path,pattern=pattern,full.name=TRUE)
    x11()
    par(col.axis="white")
    plot(c(-0.3,0.5),c(-0.4,0.45),type="n",main="Locations",xlab="",ylab="")
    par(col.axis="black")
    grid()
    for (i in seq(0,0.5,length=10)) {
      colour <- paste("grey",round(90+i*20),sep="")
      polygon((1-i)*cos(seq(0,2*pi,length=360))+0.3*i,(1-i)*sin(seq(0,2*pi,length=360))+0.3*i,col=colour,border=colour)
    }
    for (i in seq(0,80,by=10)) {
      r <- sin(pi * (90 - i)/180)
      lines(r*cos(seq(0,2*pi,length=360)),r*sin(seq(0,2*pi,length=360)),col="grey80",lwd=1,lty=2)
    }
    for (i in seq(0,360,by=10)) {
      lines(c(0,cos(2*pi*i/360)),c(0,sin(2*pi*i/360)),col="grey80",lwd=1,lty=2)
    }

    r <- sin(pi * (90 - lat.cont)/180)
    x.cont <- r * sin(pi * lon.cont/180)
    y.cont <- -r * cos(pi * lon.cont/180)
    lines(x.cont, y.cont, col = "grey30")

    for (name in locations) {
      header <- readLines(name,n=5)
      location <- substr(header[1],6,nchar(header[1]))
      colon <- instring(":",header[4])
      lon.deg.min <- as.numeric(s2n(substr(header[4],colon[1]+1,nchar(header[4]))))
      lon <- lon.deg.min[1]+lon.deg.min[2]/60
      colon <- instring(":",header[3])
      lat.deg.min <- as.numeric(s2n(substr(header[3],colon[1]+1,nchar(header[3]))))
      lat <- lat.deg.min[1]+lat.deg.min[2]/60
      r <- sin(pi * (90 - lat)/180)
      x <- r * sin(pi * lon/180)
      y <- -r * cos(pi * lon/180)
      #print(c(location,NA,lat,NA,lon))
      if (nchar(location)>4) points(x,y,pch=19,cex=0.7)
      text(x,y-0.02,location,cex=0.4)
    }
```

```
    for (station in c(90450,93700,97250,98550)) {
      obs <- KDVH4DS(station)
      r <- sin(pi * (90 - obs$lat)/180)
      x <- r * sin(pi * obs$lon/180)
      y <- -r * cos(pi * obs$lon/180)
      points(x,y,pch=19,cex=0.7)
      text(x,y-0.02,obs$location,cex=0.4)
    }
#    ealat.meta <- read.table("EALAT-list.txt",header=TRUE)
#    r <- sin(pi * (90 - ealat.meta$Latitude)/180)
#    x <- r * sin(pi * ealat.meta$Longitude/180)
#    y <- -r * cos(pi * ealat.meta$Longitude/180)
#    points(x,y,pch=19,cex=0.7)

    dev.copy2eps(file="kart.eps")
}

checkDS <- function(file="/klimadata/rasmusb/EALAT/ealat.tamYAKUTSK24959101/ds_one_AR4.ealat.tamYAKUTSK24959101.ukmo_hadcm3s1
  load(file)
  plotDSobj(ds.station)
  plotDS(ds.station$Jan)
  plotDS(ds.station$Jul)
  for (i in 1:8) {dev.copy2eps(file=paste("checkDS-",i,".eps",sep="")); dev.off()}
}




tables <- function(inflation=FALSE,period=2070:2099,absolute=TRUE,prop.chng=FALSE,pattern="ealat.tam",
                   path="/klimadata/rasmusb/EALAT",minus=8) {

  ealat.meta <- read.table("EALAT-list.txt",header=TRUE)
  ele <- switch(pattern,"ealat.tam"=101,"ealat.tax"=112,"ealat.tan" = 122)
  param <- switch(pattern,"ealat.tam"="TAM","ealat.tax"="TAX","ealat.tan" = "TAN")
  a<-list.files("/klimadata/rasmusb/EALAT_Russland",pattern="T.txt",full.names=TRUE)
  locations <- list.files(path=path,pattern=pattern)
  seasons <- matrix(c(12,1,2,3:5,6:8,9:11),3,4)
  dig      <- switch(as.character(ele),"101"=1,"601"=0)
  param    <- switch(as.character(ele),"101"="TAM","601"="RR")
  M <- rep(NA,101*4); dim(M) <- c(101,4); Q1 <- M; Q2 <- M
  m <- rep(NA,101*4); dim(m) <- c(101,4); q1 <- m; q2 <- m
  trend <- rep(NA,201*4); dim(trend) <- c(201,4)
  n <- length(locations)
  sce.2000.2040 <- rep("NA",n*4); dim(sce.2000.2040) <- c(n,4); sce.0.2000.2040 <- sce.2000.2040
  clim <- rep(NA,4*n); dim(clim) <- c(n,4)

  colnames(sce.2000.2040) <- c("Winter","Spring","Summer","Autumn")
  colnames(clim) <-          c("Winter","Spring","Summer","Autumn")

  a<-list.files("/klimadata/rasmusb/EALAT_Russland",pattern="T.txt",full.names=TRUE)

  locs <- rep("?",n)
  for (i in 1:n) {
    t <- 2000:2100
    locs[i] <- substr(locations[i],10,nchar(locations[i])-minus)
    print(paste("locs[i]=",locs[i]))
    ii <- grep(lower.case(substr(locations[i],10,14)),lower.case(substr(as.character(ealat.meta$Name),1,5)))
    if (length(ii)>0) {
      print(as.character(ealat.meta$Name[ii]))
      iii <- grep(ealat.meta$WMO[ii],a)
      obs.get <- paste("read.ealat('",a[iii],"',verbose=FALSE,param='",param,"')",sep="")
      esd <- showall(locations[i],predictand=pattern,ele=ele,plot=TRUE,path="/klimadata/rasmusb/EALAT/",
                     case.sens=TRUE,obs.get=obs.get)
      obs <- esd$plume$obs
      N <- length(esd$scen.files.a1b)
      z <- rep(NA,101*N*4); dim(z) <- c(101,N,4)
      X <- obs$yy

      for (igcm in 1:N) {
        for (is in 1:4) {
          if (ele==101) {
```

```
      y <- colMeans(esd$sce[igcm,seasons[,is],])
      clim[i,is] <- mean(obs$val[is.element(obs$yy,1961:1990),seasons[,is]],na.rm=TRUE)
    } else if (ele==601) {
      y <- colSums(esd$sce[igcm,seasons[,is],])
      clim[i,is] <- mean(rowSums(obs$val[is.element(obs$yy,1961:1990),seasons[,is]]),na.rm=TRUE)
      obs$unit <- "mm/season"
    }
    x <- esd$yy.21c
    if (ele==601) { y[y < 0] <- 0 }
    iii1 <- is.element(2000:2100,x)
    iii2 <- is.element(x,2000:2100)
    z[iii1,igcm,is] <- y[iii2]
  }
}

for (is in 1:4) {
for (it in 1:101) {
  M[it,is] <-  median(z[it,,is],na.rm=TRUE)
  Q1[it,is] <- quantile(z[it,,is],0.05,na.rm=TRUE)
  Q2[it,is] <- quantile(z[it,,is],0.95,na.rm=TRUE)
}

trendM  <- lm(M[,is]   ~ t + I(t^2) + I(t^3)+ I(t^4) + I(t^5))
trendQ1 <- lm(Q1[,is] ~ t + I(t^2) + I(t^3)+ I(t^4) + I(t^5))
trendQ2 <- lm(Q2[,is] ~ t + I(t^2) + I(t^3)+ I(t^4) + I(t^5))

good <- c(is.finite(M[,is]))
m[good,is]  <- round(predict(trendM),2)
q1[good,is] <- round(predict(trendQ1),2)
q2[good,is] <- round(predict(trendQ2),2)
  }
}

print(c(length(t),NA,dim(m)))
intv <- is.element(t,period)


for (is in 1:4) {
  if ((absolute) & (!prop.chng))   sce.2000.2040[i,is] <- paste(round(mean(m[intv,is]),dig),"+/-",
                                    round(0.5*(mean(q2[intv,is])-mean(q1[intv,is])),dig),sep="") else
  if ((! absolute) & (!prop.chng)) sce.2000.2040[i,is] <- paste(round(mean(m[intv,is])-clim[i,is],dig),"+/-",
                                    round(0.5*(mean(q2[intv,is])-mean(q1[intv,is])),dig),sep="") else
  if ((absolute) & (prop.chng))    sce.2000.2040[i,is] <-
                                    paste(round(100*mean(m[intv,is]/clim[i,is]),dig),"+/-",
                                    round(50*(mean(q2[intv,is])-mean(q1[intv,is]))/clim[i,is],dig),sep="") else
  if ((!absolute) & (prop.chng)) sce.2000.2040[i,is] <-    # not really used...
                                    paste(round(100*(mean(m[intv,is])-clim[i,is])/clim[i,is],dig),"+/-",
                                    round(50*(mean(q2[intv,is])-mean(q1[intv,is]))/clim[i,is],dig),sep="")

}

}

rownames(sce.2000.2040) <-  substr(locs,1,6)
rownames(clim) <- substr(locs,1,6)
write.table(sce.2000.2040,file=paste("Esd_",ele,"_",min(period),"-",max(period),
                         ".txt",sep=""),quote=FALSE,sep="\t")
write.table(round(clim,dig),file=paste("Clim_",ele,"_1961-1990.txt",sep=""),quote=FALSE,sep="\t")
invisible(sce.2000.2040)
}
```